

DTIC FILE COPY

4

AD-A225 968

**Basic Characteristics of Laser Heating
in Thermoluminescence and of
Laser-Stimulated Luminescence**

Final Report

ONR Contract No.: N00014-82-K-0529

Contract Period: 7/15/82 - 2/28/90

DTIC
ELECTE
AUG 30 1990
S E D
Co

**Washington
State University**

DEPARTMENT OF PHYSICS

DISTRIBUTION STATEMENT A
Approved for public release;
Distribution Unlimited

90 00 21 044

**Basic Characteristics of Laser Heating
in Thermoluminescence and of
Laser-Stimulated Luminescence**

Final Report

ONR Contract No.: N00014-82-K-0529

Contract Period: 7/15/82 - 2/28/90

REPORT DOCUMENTATION PAGE		READ INSTRUCTIONS BEFORE COMPLETING FORM
1. REPORT NUMBER	GOVT ACCESSION NO.	3. RECIPIENT'S CATALOG NUMBER
4. TITLE (and Subtitle) Investigation of Basic Characteristics of Laser Heating in Thermoluminescence and of Laser-Stimulated Luminescence		5. TYPE OF REPORT & PERIOD COVERED Final Report 7/15/82 - 2/28/90
		6. PERFORMING ORG. REPORT NUMBER
7. AUTHOR(s) P. I. Peter F. Braunlich		8. CONTRACT OR GRANT NUMBER(s) ONR N00014-82-K-0529
9. PERFORMING ORGANIZATION NAME AND ADDRESS Department of Physics Washington State University Pullman, WA 99164-2814		10. PROGRAM ELEMENT, PROJECT, TASK AREA & WORK UNIT NUMBERS Task Area: RR011-07-01 Work Unit: NR395-079 Program Element: 61153N
11. CONTROLLING OFFICE NAME AND ADDRESS Office of Naval Research 800 N. Quincy Street Arlington, VA 22217		12. REPORT DATE 7/15/90
		13. NUMBER OF PAGES
14. MONITORING AGENCY NAME & ADDRESS (if different from Controlling Office)		15. SECURITY CLASS. (of this report) Unclassified
		15a. DECLASSIFICATION/DOWNGRADING SCHEDULE
16. DISTRIBUTION STATEMENT (of this Report) Approved for public release; distribution unlimited		
17. DISTRIBUTION STATEMENT (of the abstract entered in Block 20, if different from Report)		
18. SUPPLEMENTARY NOTES		
19. KEY WORDS (Continue on reverse side if necessary and identify by block number) Thermoluminescence, Thermoluminescence Dosimetry, Laser Heating, Heat Transfer, Gaussian Beam, Optically Stimulated Luminescence, Dosimetry, Radiography.		
20. ABSTRACT (Continue on reverse side if necessary and identify by block number) See reverse side		

Table of Contents

	Page
Preface	1
Introduction	2
Part I: Laser-Heated Thermoluminescence	4
Part II: Summary of Work on CaSO ₄ :Sm	40
Publications	44
Invited Presentations	44
Patent Disclosures	45
Theses	45
List of Graduate Students and Research Personnel	45

Accession For	
Microfilm	<input checked="" type="checkbox"/>
Printed	<input type="checkbox"/>
Microfiche	<input type="checkbox"/>
Other	
Accession/	
Library Codes	
Special	
A-1	



Preface

This report summarizes the work carried out from 7/15/82 - 2/28/90 under ONR sponsorship on laser-stimulable luminescence. The effort emphasized three aspects:

1. Investigation of basic laser-stimulated luminescence phenomena such as laser-heated thermoluminescence for radiation dosimetry and optical (non-thermal) stimulated luminescence for potential application in radiation imaging and personnel dosimetry.
2. Graduate student training and interaction with guest scientists.
3. Technology transfer to U.S. industry.

Dr. Herschel S. Pilloff was the technical monitor. We are greatly indebted to him for his support and enthusiastic interest in this work, and particularly for his encouragement to apply the gained knowledge toward solutions of problems in radiation protection in U.S. industry and the DOD.

Introduction

This research program on laser-stimulated luminescence was conceived, planned, and executed with the intent to explore the basic physical principles of laser-stimulation of storage phosphors (those that retain a small fraction of the energy absorbed when exposed to ionizing radiation) and their applications in radiation dosimetry and radiography. From the outset, cross-fertilization between this research project and a simultaneous engineering development program, carried out at International Sensor Technology, Inc., (IST, Inc.) was an important aspect of the effort. Information on the physics of laser heating of two-layer structures (the phosphor layer on a substrate) influenced the design of equipment and thermoluminescence dosimeter configurations at IST, Inc. which, in turn, supplied to the ONR-sponsored program at Washington State University electronic circuit and electro-optical designs for its experimental setups. This collaboration between an academic institution and U.S. industry has been sanctioned, encouraged, and supported by ONR as it became clear that the work would yield the scientific basis for the development of a new generation of instruments and dosimeters for personnel dosimetry to be used by the U.S. Navy. The success of this approach has been extraordinary: IST, Inc. has just concluded an Advanced Development Contract for the U.S. Navy (Contract No. N60921-88-C-0085, NSWC, Silver Spring, MD), and a full scale engineering contract will be awarded to the successful bidder in September of 1990. Thus, all prerequisites for use of the new dosimetry equipment by the U.S. Navy are in place, and a purely academic research project will have been transferred to industry for production for instrumentation that is of importance for our national defense.

Finally we mention here two additional spin-offs: a two-dimensional dose mapping apparatus and a fiber-optic dosimetry probe. Both benefited greatly from the ONR supported research on laser-heated thermoluminescence. These instruments are presently

under development at IST, Inc. with Small Business Innovation and Research (SBIR) support from the National Cancer Institute.

A chronology of events in the development of all technology that is based on laser-heating of thermoluminescent phosphors is given in Table 1.

After completion of the work on laser-heated thermoluminescence we investigated non-thermal laser stimulation of inorganic phosphors that we considered to be potential candidates for dosimetric applications. This part of the effort concentrated on two materials: ZnS:Dy for use in neutron radiography and CaSO₄:Sm as the first non-thermally laser-stimulable phosphor for personnel dosimetry.

The work on ZnS:Dy was discontinued after it became clear that neither WSU nor IST, Inc. were equipped for experiments on neutron radiography and no other U.S. firm indicated any interest in the developed concept. A patent disclosure, submitted to the WSU Patent and Trademark Office was, therefore, not acted upon.

The development of the first laser-stimulable phosphor with genuine potential for applications in personnel dosimetry must be considered the basis for future work. As its laser stimulation is non-thermal, several disadvantages of laser-heated thermoluminescence may be eliminated: heating is relatively slow as compared to optical stimulation and both, binder and substrate, of a thermoluminescent dosimeter element must withstand 300-400°C. An optically stimulable dosimetric phosphor allows the construction of dosimeters using organic binders for the sensitive phosphor layer as well as polymer substrates, resulting in greater simplicity and reduced production costs.

In the following we first present the main results of the laser-heating effort in thermoluminescence dosimetry (in form of reprints of four consecutive publications) and a brief summary of the CaSO₄:Sm work together with a copy of a Master's degree thesis on this topic.

**CHRONOLOGY OF LHTLD DEVELOPMENT
U.S. NAVY SPONSORED INNOVATION BY INTERNATIONAL**

1970-1980's

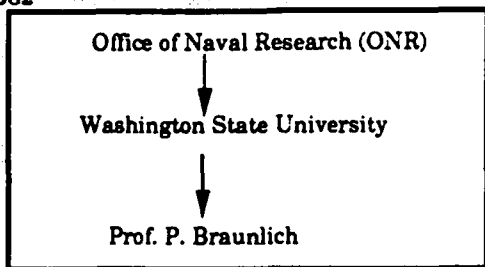
**WIDESPREAD
USE OF TLDs:**

**LIMITATIONS OF
CONVENTIONAL TLDs**

Bulky Dosimeter
Not Suitable for
Non-Penetrating Radiation
Slow Heating Cycle
Short Dosimeter Life

**DESIRABILITY OF
LHTLD IDENTIFIED**

1982



ACCOMPLISHMENTS

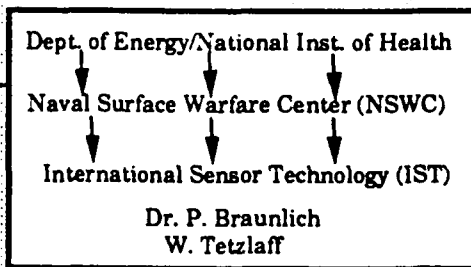
- Study of Laser Heating and Thermoluminescence
- Concept of LHTLD Developed

1982

SBIR

1987

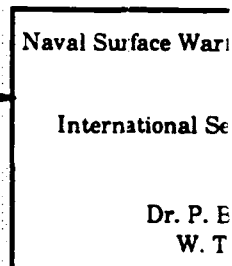
1987 **ADVANCED**



ACCOMPLISHMENTS

- Control Laser Power
- Develop Uniform Beam Power
- Fabricate Dosimeter Elements by Screen Printing
- Developed Injection Molded Dosimeter Badge
- Developed Automated Reading
- Badge Seal Development

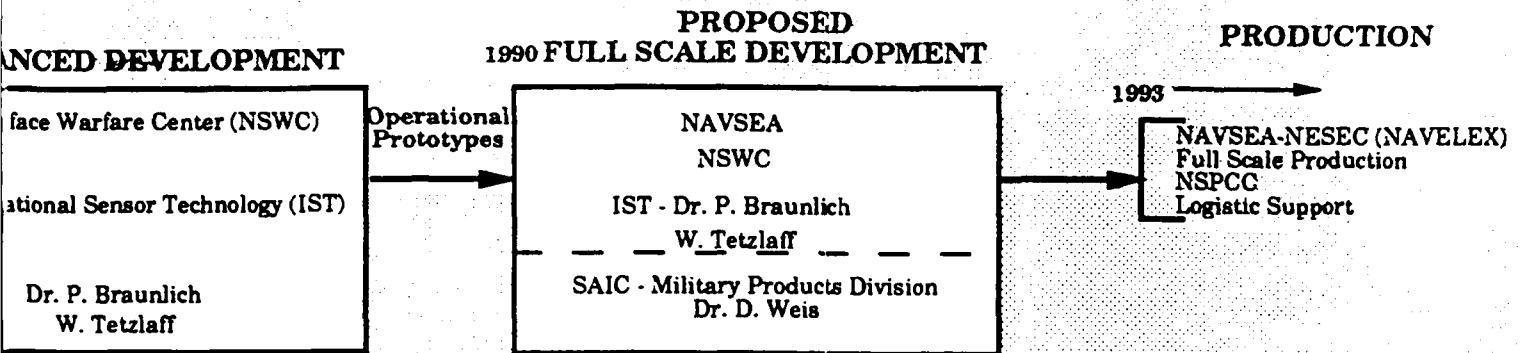
**Proof of
Concept**



ACCOMPLISHMENTS

- Low Cost Rugged
- Temperature Stable
- Photomultiplier Proofing
- Added Internal Calibration of
- Downsized Ship
- Shockproofed S
- Interchangeable Readers
- Automated Sho
- Extended Dosi
- Cycles
- Ruggedized Dos
 - Tamper Pro
 - Waterproof
 - On Board M
- Designed Fast

**DEVELOPMENT
NATIONAL SENSOR TECHNOLOGY (IST)**



ACCOMPLISHMENTS

- Most Rugged Laser
- Temperature Stable Laser Power Control
- Multiplier Tube (PMT) Shock
- Shielding
- Internal (C-14 Scintillator)
- Miniaturization of PMT
- Miniaturized Shipboard Reader
- Waterproofed Shipboard Reader
- Interchangeable Shipboard/Shorebased
- Readers
- Miniaturized Shorebased Readers
- Extended Dosimeter Lifetime >1000 Reads
- Miniaturized Dosimeter Badge
- Tamper Proof
- Waterproof
- Non-Volatile Board Memory
- Miniaturized Fast Neutron Dosimeter

GOALS

- Badge Size Reduction
- TLD Phosphor Synthesis
- Badge Parts Reduction
- Minimize Photon Angular Dependence
- Improve Proton Counter
- Accomplish Laser Low Temperature Storage
- Develop Laser/Optics Alignment Procedure
- Qualify to Full MIL-SPEC Environment
- Improve Reliability
- Improve Producability of Reader and Dosimeter
- Develop Production Document Package
- Develop LSA Documents

**CHRONOLOGY OF LHTLD DEVELOPMENT
TABLE 1**

Part I: Laser-Heated Thermoluminescence

This part of the research program commenced with a detailed study of heating a single LiF dosimeter chip and a two-layer dosimeter configuration with a TEM₀₀ mode (Gaussian beam profile) CO₂ laser beam and the corresponding thermoluminescence emission. The main results are reviewed in the paper entitled "Laser-Stimulated Thermoluminescence," presented below.

For true dosimetric applications, the laser beam must be of uniform intensity profile. Using a technique invented at IST, Inc., we continued the investigation of TL heating with a uniform square beam. This work is reviewed in the publications following the one on Gaussian beam heating.

Laser stimulated thermoluminescence

A. Abtahi and P. Bräunlich

Department of Physics, Washington State University, Pullman, Washington 99164-2814

P. Kelly

Division of Microstructural Sciences, National Research Council, Ottawa, Canada K1A 0R6

J. Gasiot

C.E.M., Université des Science et Techniques du Languedoc, 34060 Montpellier Cedex, France

(Received 2 January 1985; accepted for publication 28 March 1985)

Experimental and computational methods are presented for the complete characterization of the thermoluminescence response obtained from thermoluminescent phosphors upon exposure to localized Gaussian laser heating beams. A number of different phosphor configurations are described as examples. These include LiF:Mg,Ti (TLD-100, Harshaw Chemical Corporation) in form of chips, which are widely used in the dosimetry of ionizing radiation, and thin-layer dosimeters prepared either as self-supporting films or powder in a polyimide matrix, or on substrates of LiF single crystals or borosilicate glass. It is demonstrated that all relevant optical and thermal properties of the dosimeters can be determined by these methods and that, based on this knowledge, the expected thermoluminescence response of a given configuration can be simulated as a function of a number of experimental parameters.

I. INTRODUCTION

In recent years the feasibility of heating thermoluminescent materials with infrared laser beams has been demonstrated.¹⁻⁴ This new thermal stimulation method has received particular attention in thermoluminescence dosimetry (TLD) of ionizing radiation because it holds promise as a solution to a number of problems associated with the measurement of small doses of nonpenetrating radiation such as low-energy β rays as well as knock-on protons produced by fast neutrons in hydrogenous radiators.⁵⁻⁷ Even the imaging of spatial dose distributions of γ rays and x rays has been contemplated^{1,2} and experimentally demonstrated.⁸

The successful development of practical laser-heated TLD readers and thermoluminescence imaging devices, requires detailed knowledge of the heat transfer mechanism from the laser beam to the thermoluminescent sample and the resulting spatiotemporal temperature distribution. Then one may compute and predict the thermoluminescence response (glow curve) of the sample dosimeter for a given laser heating beam.⁹ The effects of such interrelated design parameters as laser power density, time of laser exposure, laser beam diameter and intensity profile, sample configuration and composition, and the expected incandescent background emission can be computer-simulated and the resulting glow curve compared with experimental results.

The list of experimental parameters is narrowed down to the few that presently appear important for practical applications. For example, the laser power of cost-effective modern rf or dc discharge excited CO₂ waveguide lasers or rf-excited unstable resonator lasers is limited to less than 100 W. Laser beam profiles are normally Gaussian intensity distributions or the characteristic annular cross section ("halo") that is possible with an unstable resonator cavity. Uniform beam profiles are highly desirable, but all known methods to produce such beams appear to be impractical in

TLD applications because of the associated power loss or the required custom fabrication of expensive special optics.¹⁰

Suitable dosimeter configurations are thin layers of the TLD phosphor, either in the form of a self-supporting film composed of a high temperature polymer mixture with phosphor particles, or applied to a thin substrate. Both may take the form of discrete circular spots whose diameter is smaller than the full width at $1/e$ power of the laser beam or may be prepared as continuous layers whose area is much larger than the laser beam diameter. However, even the widely used square TLD chips (e.g., the configurations supplied by Harshaw/Filtrol¹¹) or round pellets¹² can be successfully heated with a CO₂-laser beam.¹³

Small discrete dosimeters can be heated quite uniformly with Gaussian beams provided the laser photons are not too strongly absorbed (uniform heating in the direction of laser propagation). Strongly absorbing dosimeter layers (surface heating) must be thin enough that the thermal response time¹⁴ of the sample is much shorter than the total heating time required to release all trapped carriers. A necessary condition for a spatially uniform temperature rise in both cases is, of course, that the diameter of the discrete spot is much smaller than the diameter of the laser beam. Obviously, a considerable fraction of the laser beam energy is wasted in this mode of operation which, for this reason, will probably be considered only in special situations.

Continuous dosimeter layers are of practical interest because of the ease with which they can be fabricated and because of their potential usefulness in a number of the new applications mentioned above. A localized Gaussian beam can be employed to rapidly heat a small spot on the TLD layer, yielding a characteristic glow curve that is the result of the nonuniform spatiotemporal temperature distribution $T(x,y,z,t)$ produced in this way. This type of thermoluminescence response is completely different from the conventional glow curves obtained by uniform contact heating (an example is shown in Fig. 9 below). It is nevertheless very useful in

dosimetric and imaging applications of thermoluminescence.¹⁵

In this paper we present the theory of the thermoluminescence response curves generated with Gaussian laser beam profiles in a number of dosimeter configurations that are of practical importance in thermoluminescence dosimetry. The theoretical approach is verified by comparison with experimental results. In addition, experimental methods are presented for the determination of all relevant thermal and optical properties of the dosimeter materials. Thus, the thermoluminescence response of a given type of dosimeter is completely characterized and the effects of such design parameters as layer thickness, laser power and beam size, preannealing temperature and duration, substrate material and its thickness can all be assessed by computer simulation. The special case of semi-infinite LiF slab has been reported previously.⁹

II. THERMOLUMINESCENCE KINETICS FOR NONUNIFORM SPATIOTEMPORAL TEMPERATURE DISTRIBUTIONS

A. General remarks

Calculations of thermoluminescence glow curves on the basis of simple electron kinetic models and for spatially uniform heating pose no principle problems. While only special cases yield analytical solutions for the thermoluminescence intensity as a function of time or temperature, numerical solutions can readily be generated for the coupled nonlinear rate equations which describe a given trap model.^{16,17} The extreme heating rates possible with lasers have been shown not to invalidate the electron-statistical foundation (Shockley-Read statistics^{18,19}) of these phenomenological theories.⁴

Usually a number of different physically plausible electron-kinetic models will give satisfactory fits of experimental glow curves. This general lack of uniqueness renders trap-level spectroscopy by monitoring thermally simulated electron-kinetic relaxation phenomena a nontrivial task.^{16,17} Spatially nonuniform heating significantly increases the required computational effort and further complicates this situation. For this reason, laser heating techniques are explored herein for the sole purpose of assessing their utility in the dosimetry of ionizing radiation. No attempt is made to verify a given simple trap model or to extract new methods which might facilitate trap-level spectroscopy. Thus, all that is required for our purposes is one reasonably plausible model description for the thermoluminescence kinetics of a suitable phosphor heated with a laser.

The calculations presented here are based on simple Randall-Wilkins first-order kinetics.¹⁶ As the example for a typical phosphor, we choose the most widely used dosimetry material LiF:Mg,Ti (TLD-100).¹² Experimental fits of its prominent glow peaks (customarily labelled peaks 2-5) have been reported by a number of authors, most recently by McKeever²⁰ and by Vana and Ritzinger.²¹ The fact that the numerical fitting parameters, notably the trap depths and the frequency factors, differ significantly in these papers only underlines the problems associated with curve fitting as a method to obtain basic physical information from thermo-

luminescence experiments alone. We have arbitrarily selected McKeever's data for our investigations.

B. Computational approach

Having selected a group of glow peaks in TLD-100 and a suitable, albeit, not unique, fit for modeling these peaks under various experimental conditions, the main task is the calculation of the time evolution of the temperature ("heating program") for each volume element $dx dy dz$ at location (x, y, z) of the sample.

A rich literature exists in the field of laser heating of materials. For example, laser annealing of semiconductors has become an important manufacturing tool in the electronics industry.²²⁻²⁷ Laser absorption calorimetry of very transparent optical materials also requires the knowledge of the time-dependent temperature distributions produced in the sample.²⁸ Important insight in the laser damage properties of high-power metallic and dielectric mirrors and other optical components has been gained by studying the theory of laser heating.^{29,30} Comprehensive treatments of heat conduction in solids and associated boundary value problems are the texts by Carslaw and Jaeger³¹ and Ozisik.³² However, despite an extensive bibliography on laser heating, the problem of heating thermoluminescence dosimeters with a Gaussian beam turned out to be a unique new case. It is perhaps most closely related to the one solved by Bernal²⁸ who considered Gaussian beam heating of extremely weakly absorbing cylinders and semi-infinite slabs. The laser beam is, in first approximation, unattenuated when traversing the entire thickness of the slab. Unfortunately, this special case is of little interest here. Weakly absorbing thermoluminescence dosimeter layers are not suited for practical applications because of inefficient use of costly beam energy. Strong to moderate beam attenuation in the active layer is characteristic for laser heating in thermoluminescence dosimetry. However, this problem can be solved analytically by the Green's function method under the assumption that the layer is semi-infinite in radial direction (local heating of a small spot on a large area) and that no significant heat loss occurs due to convection and radiation.⁹ Convection can easily be eliminated by evacuation of the sample chamber and radiative losses are indeed small considering the fact that the maximum temperatures of interest do not exceed 700 K and the heating times are limited to a few hundred milliseconds. For these assumptions to be valid, the rate of energy absorption from the laser beam must be significantly greater than that of radiative energy loss.

The resulting spatiotemporal temperature distribution is cylindrically symmetric around the beam axis. To calculate the total thermoluminescent emission as a function of time after onset of the laser exposure, the time-dependent contributions from volume elements $2\pi r \Delta r \Delta z$ are summed by numerical integration over the radial coordinate r and the direction of laser beam propagation z . Because these heating rates are nonlinear in time, analytic solutions of the electron kinetic rate equations for each of these infinitesimal volume elements and their individual unique heating rate are unavailable even for simple first-order kinetics. Therefore, the rate equations must be solved numerically on the basis of the

individual temperature evolution of each of these volume elements and their contribution to the emission intensity $I(t)$ must be summed up.

The typical situation encountered in heating a small area of a continuous semi-infinite layer of thickness L by a Gaussian laser beam of intensity

$$I(r,z) = I_0 \exp(-r^2/w^2 - \mu z) \quad (1)$$

is schematically depicted in Fig. 1. The symbols chosen are the full width $2w$ at $1/e$ peak power of the beam, the absorption coefficient μ , the radial distance r from the axis, and the distance z from the front surface upon which the beam is incident. If the beam is turned on at $t = 0$, the temperature distribution $T(r,z,t)$ evolves as a consequence of energy absorption and thermal diffusion, resulting in a spatially resolved time-dependent thermoluminescence emission pattern $I_{TL}(r,L,t)$ similar to the special case shown in Fig. 2. These photographs were obtained by heating a highly absorbing 1-mm-thick glass slab whose back side at $z = L$ was coated with a 50- μm -thick layer of ZnS:Cu powder. Here the thermoluminescence emission $I_{TL}(r,z,t)$ is not due to direct laser heating of the phosphor itself. Instead, the thermoluminescent layer is heated by temperature diffusion through the glass. Similar experiments were described previously.² After appropriate calibration such a thermoluminescent layer can be used to measure the time evolution of isotherms during laser heating of materials. For example, the diameter of the dark center spot in Figs. 2(b) and 2(c) corresponds to the 438 K isotherm because the thermoluminescence emission of ZnS:Cu, measured by conventional uniform slow heating at a constant heating rate of 15.3 K/s, ceases at this temperature. Note that the average heating rate in the laser experiment (Fig. 2) is about the same as can be discerned from the appearance of the dark center spot at about 10 s. Other isotherms may be selected as well. For example the peak emission (region of maximum brightness in Fig. 2) corresponds to approximately 31 K. Still other emission intensities, measured relative to the peak emission, may be cho-

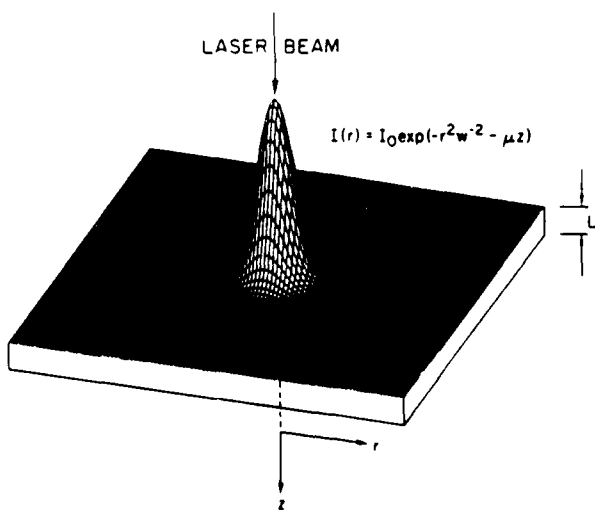


FIG. 1. Schematic representation of a Gaussian laser beam profile exposing the surface ($z = 0$) of a slab of thickness L .

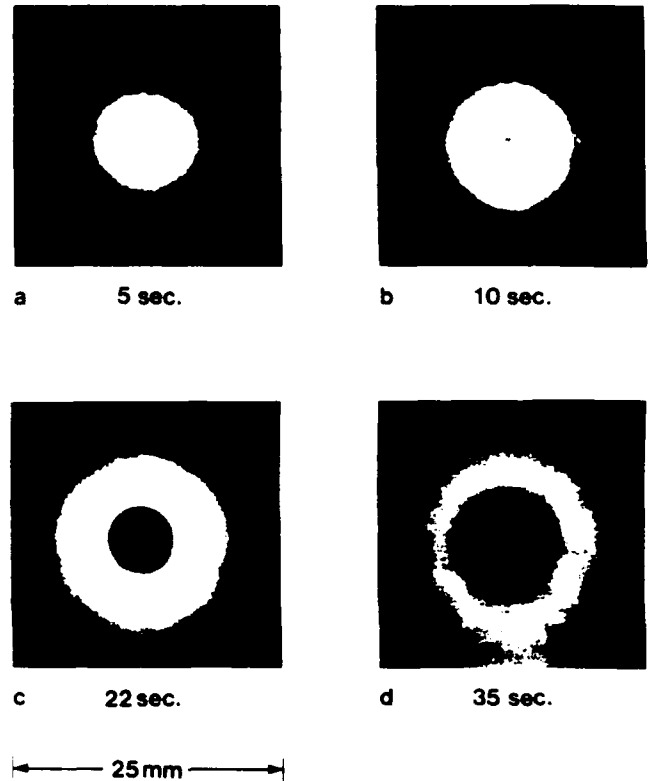


FIG. 2. Thermoluminescent emission pattern obtained from a 50- μm -thick uniform ZnS:Cu layer on a 1-mm-thick glass slab ($25 \times 25 \text{ mm}^2$). The sample was heated by a cw CO_2 laser beam of 4.3 W and 5.4-mm full width at $1/e$ peak power. The beam was directed perpendicularly at the center of the glass slab on the side opposite to the phosphor layer. The photographs were taken at the indicated times after onset of the laser exposure.

sen. Actually, the entire temperature distribution present at a given time after onset of heating can be determined by comparison of the normalized emission intensities in Fig. 2 with those of the conventional glow curve measured at approximately the same heating rate.

In dosimetry applications of laser heating the emission, integrated over the total sample volume, is measured with a photomultiplier tube without spatial resolution:

$$I_{TL}(t) = \iint dr dz I_v(r,z,t). \quad (2)$$

Here I_v is the thermoluminescence emission intensity per unit volume.

As a first step in the theory of this TL emission we calculate $T(r,z,t)$ by solving the thermal diffusion equation⁹

$$\nabla^2 T(r,z,t) + k^{-1} g(r,z,t) = \alpha^{-1} dT/dt \quad (3)$$

for the following boundary conditions.

(a) The slab is infinite in radial direction and has a thickness L .

(b) No heat loss occurs at the boundaries $z = 0$ and $z = L$, i.e., $\partial T/\partial z = 0$. This assumption is valid in vacuum in the absence of radiative heat loss.

The initial condition is $T(r,z,t) = T_0$, i.e., room temperature when the laser beam is turned on at $t = 0$. Then the temperature obtained from Eq. (3) is the actual temperature

increase above T_0 . The notation used in Eq. (3) is as follows: k = thermal conductivity, $\alpha = k/\rho c$ = thermal diffusivity, ρ = mass density, c = specific heat, $g(r, z, t)$ = laser power per unit volume present at position (r, z) during laser exposure (source function).

The case of temperature-dependent k and α is discussed in Appendix A.

Correcting for reflective loss on the front surface at $z = 0$, the source function g becomes

$$g(r, z, t) = \begin{cases} \mu(1 - R)I_0 \exp(-r^2/w^2 - \mu z) & \text{for } t > 0 \\ 0 & \text{for } t < 0, \end{cases} \quad (4)$$

where R is the reflectivity.

We solve Eq. (3) with the initial and boundary conditions stated above by the Green's function technique.³² The general solution is

$$\Delta T = T(r, z, t) - T_0 = \frac{\alpha}{k} \int_{\tau=0}^t d\tau \int_{r=0}^{\infty} r' dr' \int_{z=0}^L dz' [G(r, z, t; r', z', \tau)g(r', z', \tau)], \quad (5)$$

where G is the following Green's function:

$$G(r, z, t; r', z', \tau) = \int_{\beta=0}^{\infty} d\beta e^{-\alpha\beta^2(t-\tau) - \tau} J_0(\beta r) J_0(\beta r') \times \left(\frac{1}{L} + \frac{2}{L} \sum_{m=1}^{\infty} e^{-\alpha\eta_m^2(t-\tau) - \tau} \cos(\eta_m z) \cos(\eta_m z') \right). \quad (6)$$

Here J_0 is the zero-order Bessel function and $\eta_m = m\pi L^{-1}$. After integration over r', z' , and β , one obtains with $P = \int_0^{\infty} I(r, 0) 2\pi r dr = \pi w^2 I_0$ (total power incident on the front surface of the thermoluminescent layer at $z = 0$) the temperature distribution⁹:

$$\Delta T = \frac{(1 - R)\alpha P}{kL\pi} \int_{\tau=0}^t d\tau \frac{e^{-r^2/(4\alpha(t-\tau) + w^2)}}{4\alpha(t-\tau) + w^2} \times \left(1 - e^{-\mu L} + 2 \sum_{m=1}^{\infty} \frac{e^{-\alpha\eta_m^2(t-\tau) - \tau}}{1 + (\eta_m/\mu)^2} \times (1 - e^{-\mu L} \cos m\pi) \cos(\eta_m z) \right). \quad (7a)$$

Note again that Eq. (7a) is the temperature in excess of the initial temperature T_0 . The properties of $\Delta T(r, z, t)$ in Eq. (7a) can be readily appreciated by discussing two limiting cases for the absorption coefficient μ . Weak absorption, that is $\mu L \ll 1$, means uniform energy absorption in the z direction. The z -dependent term in the second bracket vanishes and the remaining factor $(1 - e^{-\mu L})$ is simply the fraction of the energy absorbed from the transmitted Gaussian beam. Diffusion broadens the beam profile with increasing time. Very strong absorption, that is $\mu L \gg 1$, means only a thin layer on the surface at $z = 0$ is directly heated and bulk heating occurs only by thermal diffusion. This case is of interest for certain practical dosimeter configurations.

The actual computer simulations make use of the heating rate of each volume element $2\pi r \Delta r \Delta z$, calculated from Eq. (7a):

$$dT/dt = \frac{(1 - R)\alpha P}{kL\pi} \frac{e^{-r^2/(4\alpha t + w^2)}}{4\alpha t + w^2} \times \left(1 - e^{-\mu L} + 2 \sum_{m=1}^{\infty} \frac{e^{-\alpha\eta_m^2 t}}{1 + (\eta_m/\mu)^2} \times (1 - e^{-\mu L} \cos m\pi) \cos(\eta_m z) \right). \quad (7b)$$

The four first-order differential equations which describe the independent processes of peaks 2-5²⁰ were solved together with the heating rate of Eq. (7b) by the Runge-Kutta method for each cell $\Delta r \Delta z$. Sufficient precision was obtained with $\Delta r = 2w/50$, $\Delta z = L/50$ and $\Delta t = 10^{-3} \times$ the total exposure time. The sum of the relative peak heights²⁰ was used as a measure of the total trapped electron population and each peak height was normalized by this sum to provide the initial conditions for the TL differential equations. Annealing of the lowest temperature peak no. 2 or any other is easily simulated by putting its relative height to zero.

C. Experimental procedure

The facility shown schematically in Fig. 3 was constructed for the measurement of laser stimulated thermoluminescence response curves.

A radio-frequency excited CO₂ laser (Laakmann Electro-Optics, rated at 4 W) delivers a cw beam of 1.3-mm full width at $1/e$ maximum. Together with all the required optical elements and positioners, this laser is mounted on a sturdy aluminum table.

The electromechanical shutter is the first optical element in the laser beam path. To avoid thermal distortion of the shutter blades, they are gold plated for high reflectivity. During the closed position of the shutter, the laser beam is reflected from the blades into a beam dump which simply absorbs and dissipates the laser power. The shutter has a dc power supply which is housed inside the electronic control enclosure. The electronic controlled shutter is open only to heat a sample on the sample holder or to measure by a powermeter the laser power delivered to the sample. The powermeter is mounted on a shaft which slides through the light tight box.

Following the laser beam path beyond the shutter, a 5 × beam expander is mounted on the reader table. It can be

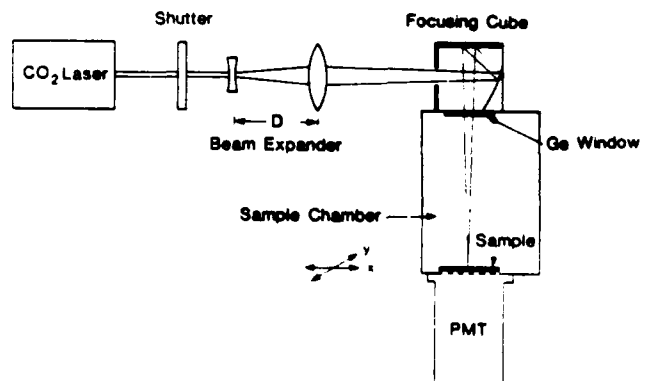


FIG. 3. Schematic representation of the laser-heated thermoluminescence reader.

adjusted to produce various beam diameters (1.5–6 mm full width) entering the focusing cube. The focusing cube deflects the beam by 90° through an AR-coated germanium window and causes it to converge on the TL sample in the light tight box. The germanium window is transparent at the 10.6- μm laser wavelength, but opaque to visible light. The beam position on the TL sample is determined by moving the sample holder with two connected x - y translation stages. The translation stages have two actuators which are driven by the Newport Corporation model 350M motor drive system and give an accuracy of the beam position up to 0.1 μm .

The TL sample is heated as it absorbs this infrared radiation from the laser. The high-power density of the focused laser beam causes the selected spot on the TL sample to be heated rapidly, while the remainder of the sample remains cool.

The TL emitted by the sample passes the sample substrate and reaches into the photomultiplier tube (PMT) below. The PMT is protected from two types of accidental exposure, one due to the laser by a glass window which will absorb the 10.6- μm laser beam, another one due to the visible light (when the sample chamber is open) by a thick aluminum slide. The PMT is an EMI type 9924B with a 1-in.-diam bialkali photocathode. The current signal from the PMT is digitized, stored, and displayed by a Data Precision 6000 Universal Waveform Analyzer (transient digitizer).

The laser TLD reader was designed to permit examination of a number of experimental parameters related to laser heating TLD, e.g., the laser power density that the sample receives, and the beam diameter which is set by mechanically adjusting the beam expander. Laser power and heating time are controlled by settings in the electronic control unit (Fig. 4).

The timing circuits in the electronic control unit consist

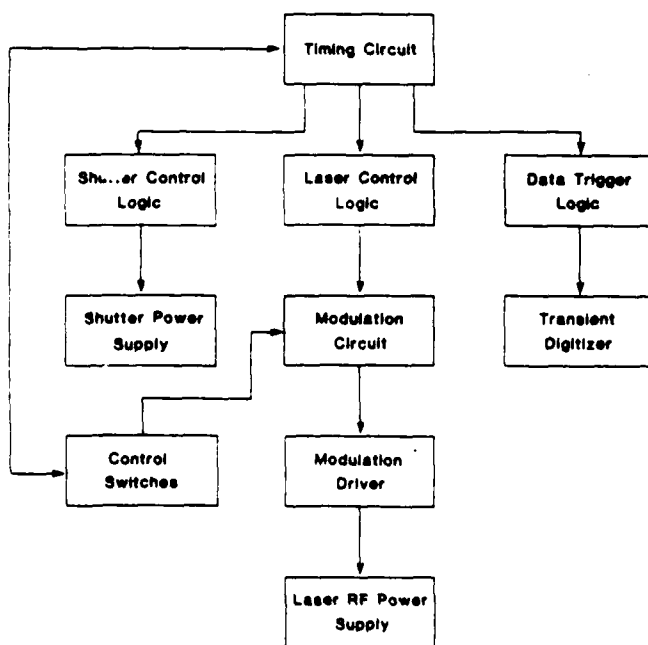


FIG. 4. Block diagram of the electronic control system for the apparatus shown in Fig. 3.

of four LM555 timers that generate four timing pulses. The first pulse drives the cycle indicator and limits read cycles to one per second. The second pulse is used to turn the laser off and open the shutter. The third pulse turns the laser on for a precise preselected timing interval. The transient digitizer is triggered at the beginning of this pulse, and the laser is turned off at its end. The fourth pulse triggers the closing mechanism of the shutter. The laser power during the third timing pulse is determined by modulation control. Whenever all four of these pulses are off, the laser operates in a cw mode at maximum output power to maintain a stable operating temperature.

The modulation circuit consists of a 10-MHz oscillator that triggers a variable length pulse generator. The modulation control is used to vary the pulse width of the resulting pulse train, permitting the laser output power to be varied over a range from zero to full power. The modulation driver amplifies the modulation signal to the 6-V pulse height required for the laser rf power supply. The shutter control signal and the data signal are both logic level signals. The 74LS series TTL logic circuits are employed for all control logic.

As will be demonstrated below (see, for example, Fig. 12), the shape of the thermoluminescence response curve depends critically on the laser beam profile in the sample plane at $z = 0$. For this reason we have given its precise measurement particular attention, using the so-called scanning knife edge method.³³

A photodetector measures the laser power not occluded by a knife edge, scanning through the beam, as a function of position. The spatial profile is then given by the first derivative of the photodetector signal with respect to the scan direction. A necessary requirement is that the mathematical form of the profile be separable in the coordinates perpendicular to and parallel to the scan directions as in the case of a Gaussian.

To check for deviations from circular symmetry, we have always scanned in two perpendicular directions. For cw lasers this procedure is readily executed by scanning at a constant rate and analog differentiation with an appropriate RC circuit.³⁴ However, for infrared lasers such as the one used in our work, thermal detectors are commonly employed to monitor the beam power. Because of their saturation characteristics they are generally not suitable for scanning knife-edge applications. Modifications of this method are required. They are shown schematically in Fig. 5. The cw beam is chopped with the electromechanical shutter³ driven by an oscillator. The oscillator output is used simultaneously as a clock for a transient digitizer (Data Precision model DP 6000) to synchronize the sampling interval with the occurrence of the signal pulse from a piezoelectric detector (Barnes Engineering model 350 PZT). In our case the shutter is opened ever 73.5 ms for 3.5 ms. The recorded detector signal during a complete scan has the appearance of a digitally recorded cw signal, exhibiting only the slow temporal structure due to increasing occlusion of the beam by the knife edge. This signal is then differentiated mathematically by the microprocessor of the DP 6000.

Examples of beam profiles obtained in this fashion are

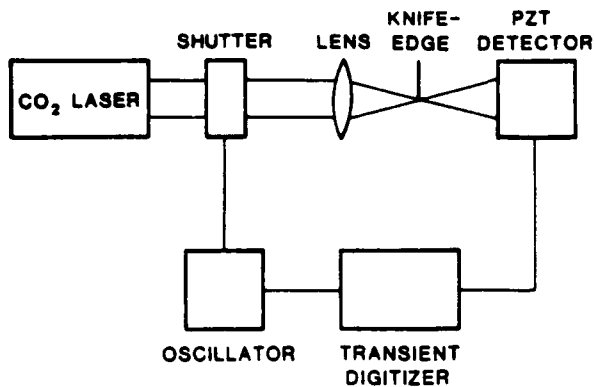


FIG. 5. Schematic arrangement for knife-edge scanning of the CO_2 laser beam profile. Note that the position of the knife-edge in the sample plane is shown here vertically because the focusing cube (see Fig. 3) is omitted for simplicity.

shown in Fig. 6. The combination of the beam expander and 5-in. focal length focusing cube afforded variations of the laser spot size in the sample plane between 0.3 and 2.22 mm. The long focal length of the cube and the maximum laser beam penetration depth in our samples of less than $300\ \mu\text{m}$ implies that the laser beam profile is independent of the z direction.

In the following sections we present experimental results obtained with a number of different dosimeter configurations and comparisons with theoretical calculations.

III. RESULTS AND DISCUSSION

Case 1: LiF:Ti:Mg chip

Laser heating of microcrystalline hot-pressed TLD-100 dosimeter material produced by the Harshaw/Filtrol Corporation¹¹ is of interest as it is widely employed in routine personnel dosimetry. From a theoretical point of view this case is important because of the rather modest absorption coefficient ($\mu = 40\ \text{cm}^{-1}$) of LiF for $10.6\ \mu\text{m}$ photons. The laser beam penetrates $250\ \mu\text{m}$ ($1/e$ attenuation depth) into the $900\text{-}\mu\text{m}$ -thick chip. As it turns out, none of the previously reported solutions of the heat flow equation [Eq. (3)] cov-

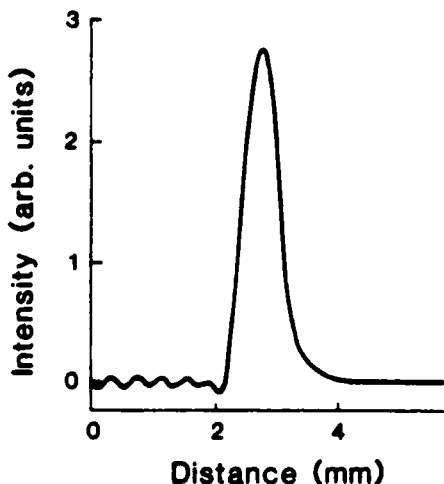


FIG. 6. Example of a typical nearly Gaussian spatial profile obtained for the CO_2 laser beam at $z = 0$ (see Fig. 1).

ers this situation in conjunction with a Gaussian heating beam.

Unfortunately only small chips ($3 \times 3 \times 0.9\ \text{mm}^3$) are commercially available and, therefore, care has to be taken not to violate the assumption of a semi-infinite medium (see Sec. II) when comparing computed with experimental results. In practice this can be done by choosing a beam diameter that is much smaller than the width of the sample and by limiting the total exposure of the laser heating beam to a time during which the sample edges have not yet been heated by thermal diffusion. In order to reach, during this time, in the center of the exposed area the highest temperature peak (peak no. 5), the power density in the beam center must exceed a minimum value. In essence this requirement means that a substantial part of the chip volume must be heated to above the maximum temperature for which TL emission will still occur before the edge areas experience any temperature increase by thermal diffusion. We have performed these experiments successfully with beam diameters around 0.084 cm and approximately 5-W power. Under these conditions a 300-ms exposure time raised the temperature at the edges by only a few degrees K above room temperature. Continued exposure to the heating beam beyond this time resulted in heat pileup in the chip and eventual increase of the temperature of the total sample to above 700 K, a situation not covered by the theory presented in Sec. II B. However, these experiments are perhaps important as they indicate that entire TLD-100 or similar chips can indeed be heated with an appropriate laser beam so as to measure the total thermoluminescence emission. In fact, we have been able to heat these chips to 600 K within about 2 s with a 2.5-mm-diam beam of approximately 3-W power.

The temperature distribution established at the end of the exposure (300 ms) of a LiF chip to a 0.084-cm full width at $1/e$ maximum of 4.93 W power is depicted in Fig. 7. Isotherms, calculated from Eq. (7a), are shown for temperatures corresponding to the peak temperatures of peaks 2–5 (383, 421, 457, and 483 K, respectively). The volume inside the 483 K isotherm is heated to temperatures for which thermoluminescent emission from peaks 2–4 has ceased at 300 ms. Figure 7 illustrates the nonuniformity of both the temperature distribution and, albeit indirectly, the thermoluminescent emission pattern.

We have made no attempts in our experiments to measure the spatial distribution of the time-dependent thermoluminescence response of the TLD-100 chip to the Gaussian heating beam. Instead the total emission $I_{\text{TL}}(t)$ was monitored with a photomultiplier tube and compared with computations performed with the theory outlined in Sec. II B. The results are presented in Fig. 8 for a TLD-100 chip that was preannealed to 373 K for 10 min in order to remove peak 2. This type of thermal treatment after exposure to the ionizing radiation and before measuring the thermoluminescence glow curve is customary in dosimetry applications of this material. The agreement between the calculated and experimental glow curve is rather satisfying in light of the uncertainties concerning the exact electron-kinetic model description of the thermoluminescence emission from this material and the fact that the TLD-100 chip is not a single crystal as

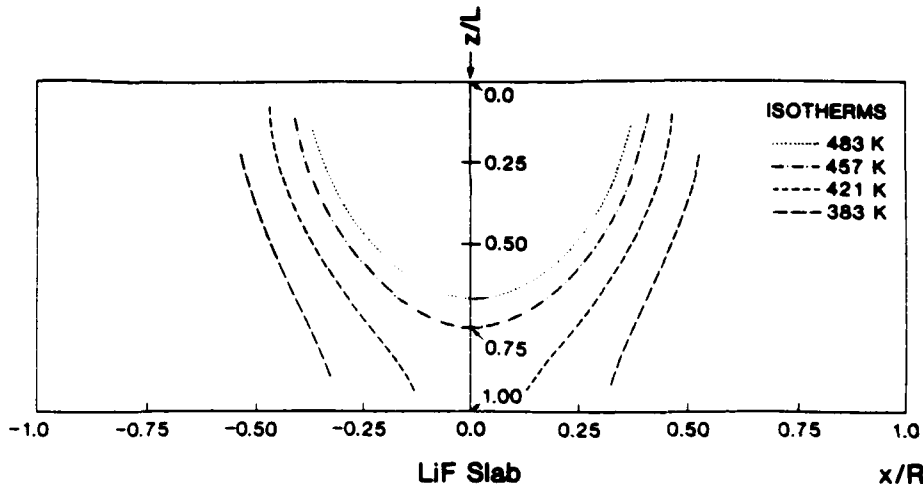


FIG. 7. Temperature distribution established after heating a small LiF slab of area $3 \times 3 \text{ mm}^2$ and thickness $L = 0.9 \text{ mm}$ for 300 ms. A Gaussian laser beam of 4.93-W power and 0.84-mm full width impinges on the center of the slab at $z/L = 0$. The calculations were performed with Eq. (7b) and $k = 0.0275 \text{ W/cm K}$, $c = 1.56 \text{ W s/g K}$, $\rho = 2.635 \text{ g/cm}^3$, and an absorption coefficient for $10 \mu\text{m}$ of $\mu = 40 \text{ cm}^{-1}$.

assumed in the calculations. An additional uncertainty stems from the rather strong temperature dependence of the thermal conductivity k . According to Men *et al.*,³⁵ k decreases with increasing temperature approximately as T^{-1} . The calculated curve shown in Fig. 8 was obtained with $k = 0.0275 \text{ W/cm K}$, which is approximately one third of the value measured for a single crystal at room temperature. We have also performed the calculation with an exact solution of the heat flow equation with $k(T) = k_0 T_0/T$ using Kirchhoff transformation techniques (see Appendix A). However, no significant improvement in the agreement between measured and calculated thermoluminescence response curves was obtained, perhaps indicating that unaccounted for experimental factors influenced the results more than an improved theory of heat conduction. We suspect that the microcrystalline "ceramic" nature of the sample and the roughness of the unpolished surface caused some deviations from the implicit assumption that the optical and thermal properties of this material are very close to those of single-crystalline LiF. Scattering of the laser light probably results in some broadening of the Gaussian beam profile inside the chip, and the thermal conductivity may be lower than that of a single crystal. In addition, it is well known that, in order to reproduce the exact relative peak heights of peaks 2–5 of the TLD-100 phosphor as used in Ref. 20, the annealing procedure must be reproduced exactly.¹² Slight deviations might have been present as compared to those used by McKeever,²⁰ resulting in small peak height difference particularly of the low-temperature peaks which significantly influence the thermoluminescence response curve obtained by Gaussian beam heating (see Case 4 of this section).

Case 2: Polyimide foil loaded with LiF:Mg,Ti powder

Thin dosimeters are desirable for applications in the dosimetry of low-energy β rays. We have experimented with 84- μm -thick foils of polyimide (Kapton, DuPont) which were produced by thoroughly mixing TLD-100 powder (grain size 20–30 μm) with liquid polyimide and spreading this slurry uniformly onto glass slides. After curing for sev-

eral minutes at 373 K and subsequently for 1 h at 573 K, the translucent yellow film was removed by immersion in water. Correcting for the weight loss during the polymerization process, the powder-polyimide weight ratio of the dry foil was about 2:1.

Pieces of $2.5 \times 2.5 \text{ cm}^2$ size were mounted in metal frames and exposed to γ rays from a ^{60}Co source. The absorbed dose was 26 Gy. Following a 10-min preanneal at 373 K, the thermoluminescence response curves were measured for a fixed laser power of 4.78 W and various laser spot sizes ranging from 0.039 to 0.098 cm diameters. A family of curves measured under these conditions is depicted in Fig. 9. Several different sites on the same sample were heated for each laser spot size to assess sample uniformity and laser stability.

All experiments were performed to test the validity of the theory presented in Sec. II B rather than to fabricate

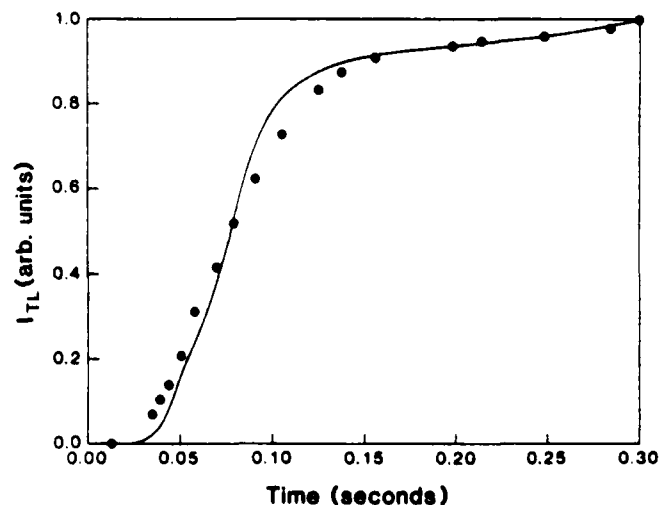
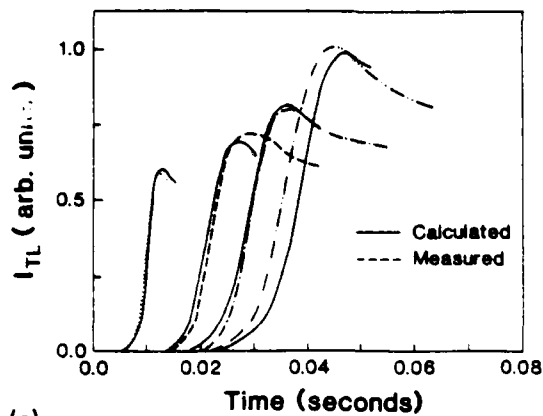
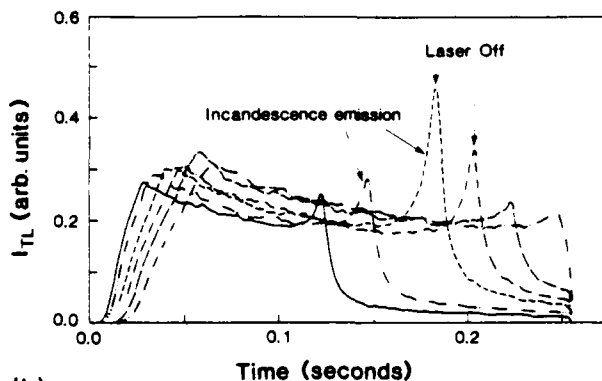


FIG. 8. Measured and calculated (solid line) thermoluminescence response curves obtained from the LiF:Mg, Ti (TLD-100) chip of Fig. 7 after x-ray exposure. The calculations were performed with Eq. (7b) and the first-order electron kinetic parameters (frequency factor, trap depth) determined by McKeever²⁰ for peaks 3–5 of this thermoluminescent phosphor. Peak 2 was removed by 10-min preannealing at 373 K.



(a)



(b)

FIG. 9. (a) Measured and calculated (solid line) thermoluminescence response curves obtained after x-ray exposure of a 84- μm -thick polyimide foil loaded with LiF:Mg,Ti (TLD-100) particles of 20–30 μm grain size at a polymer-powder weight ratio of 1:2. The curves were measured with a 4.7-W CO_2 laser beam of full widths (from left to right) of 0.39, 0.62, 0.77, and 0.985 mm. The calculations were performed with Eq. (8) and $B = 26 \text{ K cm}^2/\text{s}$ [see Eq. (9)] which was determined by the incandescence emission method (Appendix B) at this laser power. The thermal diffusivity of the polyimide-LiF composite was found to be $\alpha = 0.0175 \text{ cm}^2/\text{s}$ by the best fit of the calculation to a series of measured curves obtained with various laser spot sizes but otherwise identical conditions. (b) A set of thermoluminescence response curves obtained with an identical sample as the one used in (a) except for longer heating times, which were increased to demonstrate the occurrence of incandescence emission. Each curve drops off sharply upon turning off the laser beam. Laser power: 4.75 W. Laser beam diameter $2w$ (mm) (from left to right): 0.899, 0.942, 0.985, 1.024, 1.063, and 1.102.

viable dosimeters. For example, Kapton absorbs quite strongly the TLD-100 thermoluminescent emission centered around 400 nm and, therefore, a foil of this type is rather insensitive as a dosimeter. Nevertheless, important information on the energy transfer from a laser beam to a sample of this type and the resulting thermoluminescence response can be gathered and eventually applied to Kapton foils loaded with TL powders other than LiF.

The TLD-100 loaded Kapton foil does not strongly absorb 10.6- μm photons. Yet, direct measurement of its absorption coefficient is not trivial because of the photon scattering off the LiF particles dispersed in it. Since the foil is quite thin and LiF has a rather small absorption coefficient for 10.6- μm photons, one can safely assume that the heat deposition is independent of z throughout the entire thick-

ness L . However, scattering introduces an element of uncertainty whose influence on the agreement between theory and experiment can only be estimated by the comparison of measured and calculated thermoluminescence response curves. This case of relatively weak absorption is characterized by $\mu L \ll 1$. As a result, Eq. (7a) becomes independent of z :

$$\Delta T = B \int_{\tau=0}^t d\tau \frac{e^{-\tau/(4\alpha t - \tau) + w^2}}{4\alpha(t - \tau) + w^2}, \quad (8)$$

with

$$B = \frac{(1 - R)(1 - e^{-\mu L})}{\pi \rho c L} P. \quad (9)$$

In attempting to calculate the family of curves in Fig. 9(a), the problem of determining the thermal and optical properties of the sample that enter Eq. (8) presents itself. For example, it is not immediately possible to obtain the relevant averaged thermal conductivity k for such a heterogeneous mixture from the known values of its components. Also, the total absorbed power $P(1 - R)(1 - e^{-\mu L})$ is difficult to determine without a suitable calorimeter, while the averaged specific density ρ and heat capacity c can be calculated in principle from the values of the components.

However, the quantity B defined by the entire parameter combination in Eq. (9) can be measured by exploiting the normally undesired onset of incandescent emission that is observed when the sample is exposed to the laser beam significantly beyond the occurrence of the glow curve maximum [see Fig. 9(b)]. We have developed a method for this task that is based on Planck's law of blackbody emission. It makes use of the exponential time dependence of this emission when it is measured for a narrow wavelength interval whose center wavelength, $\bar{\lambda}$ has to be selected in the red or better yet in the infrared so as to not destroy the sample by overheating it. Also, the experiment has to be performed with significantly higher laser power densities as compared to the ones used in the thermoluminescence experiments in order to assure that the condition $4\alpha t \ll w^2$ is fulfilled so that measurable incandescent emission is generated before the onset of thermal diffusion. Under this condition the temperature rise of the heated spot is linear in time as can be seen from Eq. (8).

$$\Delta T = T - T_0 = Bt/w^2, \quad (10)$$

and it can be shown (see Appendix B) that the so-measured incandescent emission intensity I obeys the relation

$$\left(\frac{\partial I}{\partial t}\right)/I = [a/(Bt/w^2 + T_0)^2](B/w^2), \quad (11)$$

where $a = hc/\bar{\lambda}k$ and T_0 is the initial temperature. The quantity B can be calculated by carefully measuring the laser spot size $2w$ and dI/I as a function of time. Details of this method are presented in Appendix B.

For the above-mentioned TLD-100-loaded Kapton foils B/P was found to be 5.53 ($\text{K cm}^2/\text{J}$). With this knowledge and the known laser power the thermoluminescence response curves of Fig. 9(a) can be calculated from Eq. (8) and the computational procedure for glow curves obtained with locally non-uniform heating as described in Sec. II. This was done by normalizing a single member of a set of curves mea-

sured for different laser beam diameters $2w$ and selecting a value for the unknown thermal diffusivity α so as to obtain the best fit for all members of the set. Usually a rather good fit is possible for the curves measured with large power densities of the laser beam (e.g., in the present case smaller spot sizes for the fixed laser power of 4.70 W). Larger spot sizes tend to yield computed curves that rise later than the experimental ones and are steeper prior to reaching the maximum. Perhaps the scattering of the laser light from the LiF grains, disregarded in our computations, and the associated distortion of the laser beam profile may be a reason for this discrepancy. The value obtained for the thermal diffusivity $\alpha = 0.0175 \text{ cm}^2/\text{s}$ appears reasonable in light of the values for LiF ($0.02743 \text{ cm}^2/\text{s}$) and Kapton ($0.001 \text{ cm}^2/\text{s}$).

In closing this discussion of the powder-loaded Kapton foils it may be of interest to mention that the measurement of laser-heated TL glow curves and the developed computational procedure presented in this work point to a new method for the determination of the thermal properties of otherwise difficult to measure thin-foil TLD dosimeters.

Having completely determined the thermal and optical properties of a given dosimeter of this type, it is relatively straightforward to simulate its thermoluminescence response as a function of other experimental parameters such as laser power, beam diameter, foil thickness, preannealing temperature, and duration and the like. As an example, Fig. 10 shows the dependence on the laser power of the sample from Fig. 9(a) for a fixed beam diameter $2w = 0.062 \text{ cm}$. Thus, the techniques are now available for the optimization of dosimeter designs for the use in laser-heated thermoluminescence dosimetry readers.³

Case 3: Thin LiF:Mg,Ti phosphor layer on a glass slab: (a) Heating beam on layer

Another dosimeter configuration of potential importance for laser-heated thermoluminescence dosimetry is a thin TL phosphor layer on a substrate that is transparent for

the emitted thermoluminescence photons. In this arrangement the heating beam may be directed so as to expose a small spot of the sample on the side that is covered with the active layer and the thermoluminescent emission is monitored with a photon detector on the opposite side. The substrate may be chosen according to its absorption coefficient for the photons of the heating beam. For example BaF, LiF, and sapphire or glass are materials having absorption coefficients increasing in that order. Assuming the phosphor layer is sufficiently thin and composed mainly of TLD-100 phosphor powder, little energy is transferred from the $10.6\text{-}\mu\text{m}$ beam using a BaF substrate. However, useful thermoluminescence response curves are obtained with a single-crystalline LiF substrate (see Fig. 11). The most efficient utilization of the laser beam energy is achieved by a highly absorbent substrate such as common borosilicate glass. The thermoluminescence response of such a dosimeter configuration is the rather complex result of both direct and indirect (via absorption by the glass and subsequent diffusion) heating of the phosphor. Both, its optical properties at $10.6\text{-}\mu\text{m}$ as well as its thermal characteristics, are due to the contributions of the individual properties of both components in an unknown fashion and are for this reason difficult to measure. However, by applying a layer that is considerably thinner than the substrate and considering the fact that this layer does only moderately absorb the laser photons, heating is mostly indirect via diffusion from the strongly absorbing glass surface. Therefore, one can assume that the thermal diffusivity α of the dosimeter is very close to that of the glass ($\alpha = 0.0075 \text{ cm}^2/\text{s}$). In fact, it should be slightly higher than that of lime glass because of the contribution to the "configuration-averaged" α from the LiF content of the phosphor layer. We have performed all calculations (see below) of the thermoluminescence responses of thin-layer dosimeter configurations which use borosilicate glass substrates with the value of $\alpha = 0.01 \text{ cm}^2/\text{s}$ (glass composition: 64% silicon dioxide, 13% alkali oxides, 8% boron oxide, and 15% other

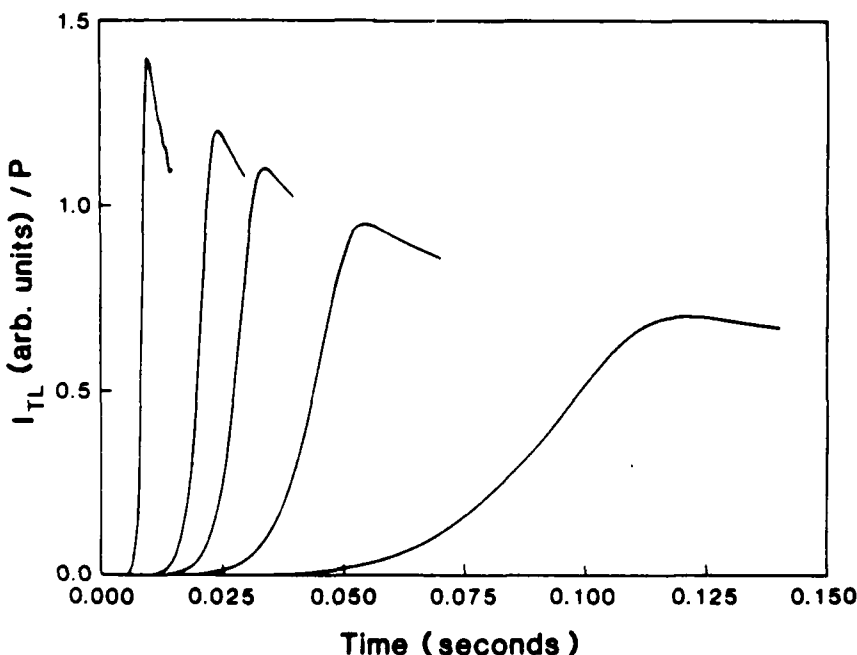


FIG. 10. Example of calculated dosimeter performance. The sample is the self-supported polyimide-powder foil from Fig. 9, all optical and thermal properties being identical. The calculations were carried out for a fixed laser spot size at 0.62 mm and laser powers P of 10, 5, 4, 3, and 2 W. Note that for clarity these thermoluminescence response curves are scaled by dividing the TL intensity by a numerical factor equal to the laser power in W.

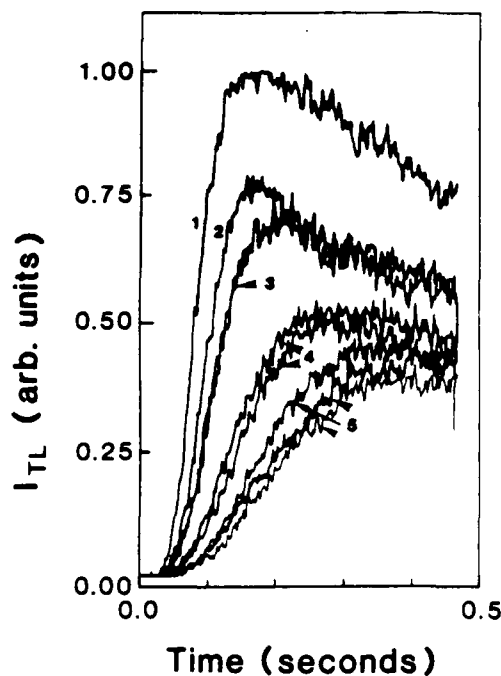


FIG. 11. Thermoluminescence response curves measured from a uniform LiF:Mg,Ti layer (thickness: 3.7 mg/cm^2 , $20\text{-}\mu\text{m}$ grain size, Dow Corning 805 silicone binder) on a 0.15-cm -thick nonthermoluminescent LiF single crystal of $25 \times 25 \text{ mm}^2$ area. Laser power: $P = 4.95 \text{ W}$. Laser spot size $2w$ (in mm): (1) 0.326 , (2) 0.327 , (3) 0.330 , (4) 0.336 , (5) 0.340 mm. To check the reproducibility of the measurements, several thermoluminescence responses from different sites on the sample were measured for otherwise identical conditions. Repeated measurements are shown here only for the largest three of the five different spot sizes chosen for this experiment.

oxides). The only parameter combination not known for this type of dosimeters is B [see Eq. (9)], which is obtained by the best fit of calculated and measured TL response curves.

We have performed experiments with thin uniform TLD-100 powder layers in a silicone binder on 0.159-mm -thick borosilicate glass microscope cover slides. An example of such a family of glow curves measured with a fixed laser power and for various laser spot sizes is presented in Fig. 12. A $25 \times 25 \text{ mm}^2$ slide was coated with a $51\text{-}\mu\text{m}$ -thick layer of LiF (TLD-100) powder (grain size between 30 and $40 \mu\text{m}$) in a silicone binder (cured weight ratio 2:1) and exposed to 50-kV x rays. After 10-min preanneal at 373 K to remove peak 2,²⁰ well-separated areas on this sample were exposed to laser heating pulses of 4.45 W power and spot sizes of full widths ranging from 1 to 2 mm . In order to avoid the onset of incandescent emission from the center of the exposed spot the exposure times were adjusted according to the power density, ranging from 100 to 250 ms . From the best fit of the computed curves to these measurements B was found to be $20 \text{ K cm}^2/\text{s}$ for the laser power stated above.

With this value of B other series of thermoluminescence response curves for this type of dosimeter can readily be generated. For example the influence of the laser power P for various spot sizes or the thickness L of the sample can be studied by computer simulation in order to arrive at an optimal dosimeter design for a given available CO_2 laser. An example is presented in Fig. 12(b) which demonstrates rather

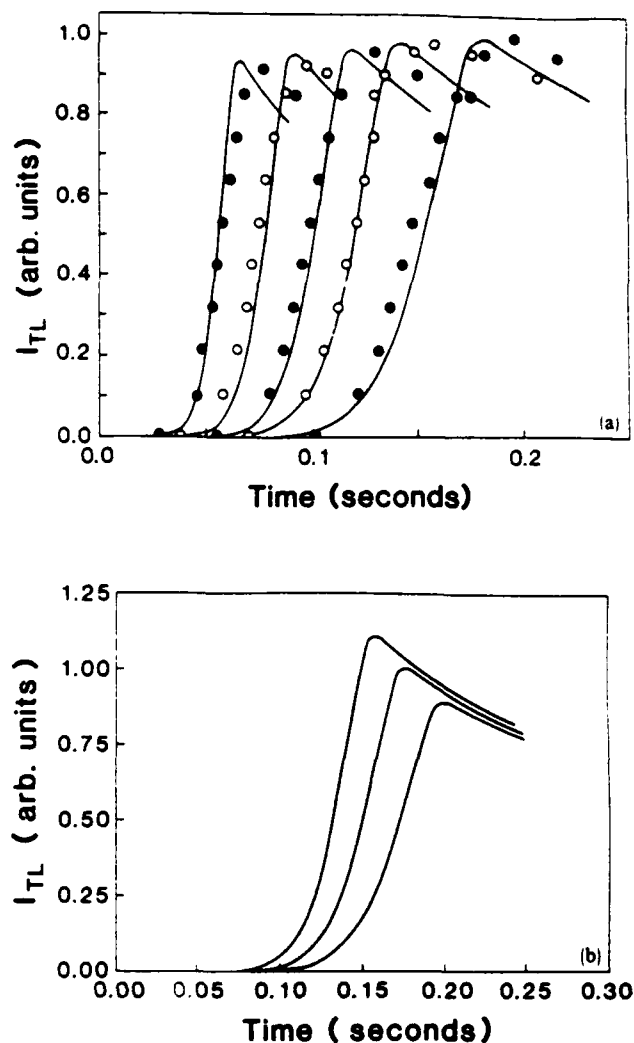


FIG. 12. (a) Thermoluminescence response curves measured with a 4.45-W laser beam by heating the phosphor-coated side of a 0.159-mm -thick glass slab after x-ray exposure. The $51\text{-}\mu\text{m}$ -thick coating consisted of TLD-100 powder (grain size $30\text{--}40 \mu\text{m}$) in a Dow Corning 805 silicone binder (2:1 weight ratio). The solid lines are curves computed from Eq. (7b) and the first-order electron kinetic parameters determined by McKeever²⁰ for peaks 3-5. Peak 2 was removed by a 10-min preanneal at 373 K . With the known thermal diffusivity $\alpha = 0.01 \text{ cm}^2/\text{s}$ the parameter B was determined by fitting a family of curves obtained for the following full widths $2w$ (mm) (curves from right to left): 2.03 , 1.83 , 1.65 , 1.45 , 1.24 , respectively. (b) Computed thermoluminescence response curves for various laser powers. The sample is identical to that of (a). The laser spot size $2w$ is 1.944 mm and the laser powers (curves from left to right) are 4.895 , 4.45 , and 4.005 W , respectively.

large changes in the peak location of the thermoluminescence response curves when varying the laser power by only 10% , indicating the necessity to use a highly stabilized laser beam for applications of laser heating in thermoluminescence dosimetry.

Case 4: Thin LiF:Mg,Ti phosphor layer on a glass slab: (b) Heating beam on glass side opposite the layer

It is of course also possible to heat the active thermoluminescent layer through the substrate. Choosing again a relatively thin microscope cover slide interesting thermoluminescence response curves from a TLD-100 phosphor layer

were obtained. Compared to those measured by frontal heating with the same laser power and beam diameter, they all peak at a later time because diffusion through the strongly absorbing substrate is now the only mechanism of heat transfer. At the same time the effected spot size is considerably larger.

A series of curves measured with a laser power of 4.18 W and spot sizes ranging from 1.65 to 2.13 mm full width is shown in Fig. 13 for the same sample used in the experiments of Fig. 12. The theoretical curves were again computed from Eq. (7b) with an experimentally determined value for the parameter combination $B = 16.75 \text{ cm}^2/\text{s}$. The best fit was obtained with a thermal diffusivity of $\alpha = (7.8 \pm 0.5) \times 10^{-2} \text{ cm}^2/\text{s}$. The calculated dependence of the thermoluminescence response on the laser power for a spot size of 1.65 mm is plotted in Fig. 14 together with curves calculated for a fixed power and spot size and different sample thickness L .

We have used the same sample in an attempt to study the effect of preannealing on the thermoluminescence response curve. These experiments are not just a trivial repetition of what has been done before by many authors to find the appropriate treatment for removal of rapidly fading low-temperature glow peaks prior to the dose measurement. Because the temperature distribution is nonuniform when a semi-infinite slab is heated by a localized beam of Gaussian profile, uniform preannealing effects the response curve much more severely than the conventional glow curve. This becomes obvious by careful examination of the photographs of Fig. 2 which may be considered as a "coded" temperature distribution in the emitting layer for the various times after onset of the laser exposure. Imagine ringlike surface areas between two adjacent isotherms of a given small tempera-

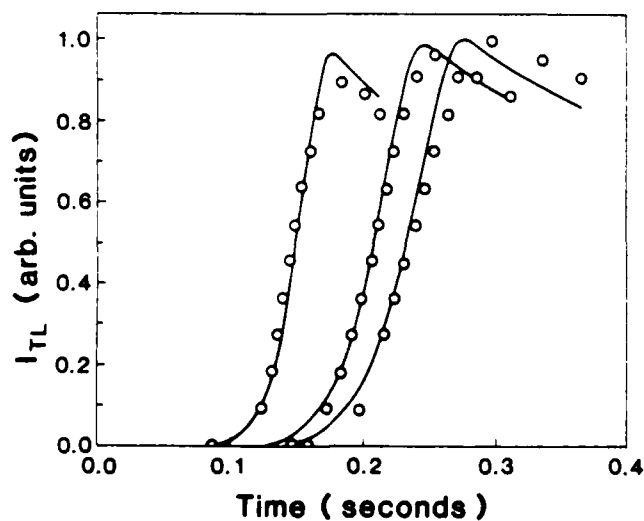


FIG. 13. Thermoluminescence response curves of the sample from Fig. 12, however, the laser heating beam impinges onto the side opposite to the phosphor-coated one. Thermal diffusion through the thin glass slab is now required to produce the thermoluminescent emission. With the known thermal diffusivity of this sample [see Fig. 12(a)] the B parameter [Eq. (9)] was determined to be $16.5 \text{ K cm}^2/\text{s}$ at $P = 4.18 \text{ W}$ by the best fit of computed curves to the entire series of curves measured for different laser beam widths $2w$. Again, peak 2 of TLD-100 was removed by annealing. The solid lines are the curves computed with Eq. (7b) and on the basis of first-order electron kinetics and the following measured beam widths $2w$ (mm): 1.65, 1.994, 2.13, respectively.

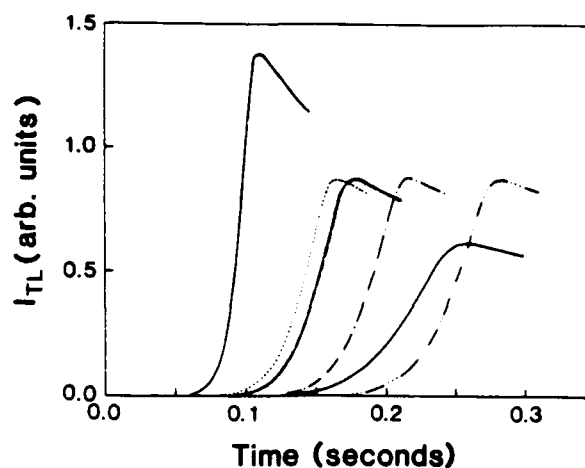


FIG. 14. Thermoluminescence response curves of the sample from Fig. 13 computed from Eq. (7b) for various laser powers P and total sample thicknesses L and fixed spot size $2w = 1.65 \text{ mm}$. Again it was assumed that peak 2 of the TLD-100 phosphor was removed by preannealing. The solid curves were calculated for $L = 0.210 \text{ mm}$ and the following laser powers (from left to right): 6.27, 4.18, and 3.125 W. The dashed curves demonstrate the effect of the total thickness L by increasing the substrate thickness only (fixed phosphor layer thickness of 0.051 mm). The calculations were performed with a laser power $P = 4.18 \text{ W}$ and the following total thicknesses L (from left to right): 0.105, 0.210, 0.420, and 0.630 mm.

ture difference. At the perimeter of the emission pattern, which is at a low temperature, the emission from such a ring is due to the low temperature peaks of the conventional glow curve. A ring of the same temperature difference, but located closer to the center, emits at the same time at a higher temperature. Assuming for the sake of simplicity identical brightness of these two areas, their contribution to the total emission (monitored with a detector and without spatial resolution) is proportional to the square of their respective radii. Removing the low temperature glowpeaks by uniform preanneal treatment affects the outer and, thus, larger emitting area and consequently the strongest contributions to the emission at that time. Figure 15 is an illustration of this phenomenon. Three thermoluminescence response curves are shown measured with a laser power of 3.63 W and a spot size of 1.6-mm $1/e$ power diameter. The sample is the same as that used to produce the curves of Fig. 13. A 373 K preanneal of only 5 min, which is known to remove the low-intensity peak 2 of the conventional glow curve²⁰ has a rather large effect on the thermoluminescence response curve measured with Gaussian laser beam heating. Preannealing at the same temperature for 10 min has almost no measurable effect on peaks, 3, 4, and 5 of the conventional glow curve while the difference can still be detected in curve c of Fig. 15. We refrain here from reporting preannealing measurements and computer simulations performed with all the sample types used in our investigations. Instead we restrict ourselves to pointing out that in practical dosimetry applications of laser heating continuous dosimeter layers with Gaussian beam profiles¹⁵ great care has to be taken to reproducibly preanneal the samples. In addition, fading of the information on absorbed doses stored in the thermoluminescence dosimeter will cause a similarly enhanced error as compared to conventional contact heating.

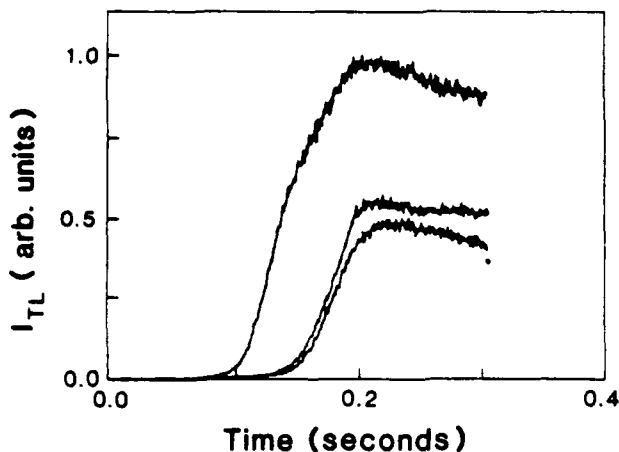


FIG. 15. Effect of preannealing for 10 min at 373 K on the thermoluminescence response curves obtained from the sample of Fig. 12 by heating it through the glass with $P = 3.63$ W and a laser spot size $2w = 1.6$ mm. The first curve (on the left) is obtained without annealing immediately after exposure of the sample to 50-keV x ray for 4 min. The other two curves represent the TL response after 5- and 10-min preannealing at 373 K, respectively.

IV. CONCLUSIONS

We have presented the theory of thermoluminescence response curves generated with Gaussian laser beam profiles for a number of practical and interesting dosimeter configurations, and we have verified our theoretical approach by direct comparison with experiment. We have also shown that by computer simulation one can assess the effects of such design parameters as layer thickness, laser power and beam size, preannealing temperature and duration, substrate material and its thickness.

The extremely fast heating rates ($> 10^4$ K/s) which can be obtained by laser heating versus that of conventional contact heating in solid-state dosimetry (~ 1 K/s) and the reduced amount of phosphor required in our thin film configuration indicate quite clearly that the techniques which we have developed and presented herein while of interest in their own right will be of significant practical importance.

ACKNOWLEDGMENTS

The authors are indebted to S. C. Jones, W. Tetzlaff, and M. deMurcia for their valuable contributions in the early stages of this project, which was sponsored by the Office of Naval Research under Contract No. N00014-85-K-0529.

APPENDIX A

When the thermal conductivity varies with temperature, the nonlinear differential equation of heat conduction (compare with Eq. 3) can be written as

$$\nabla [k(T)\nabla T] + g(r,z,t) = \rho c \partial T / \partial t, \quad (\text{A1})$$

where the thermal conductivity k and the thermal diffusivity α are assumed to be temperature dependent; but the heat source function $g(r,z,t)$ does not depend on temperature.

Equation (A1) can be linearized by a transformation which involves a change of the dependent variable. This

method is called the Kirchhoff transformation.³² The new variable of transformation U is defined as

$$U = \int_{T_0}^T \frac{k(T')}{k_0} dT'$$

or by

$$\frac{\partial U}{\partial T} = k(T)/k_0, \quad (\text{A2})$$

where T is a reference temperature and k_0 is the value of $k(T)$ at T_0 . Upon substitution, Eq. (A1) becomes

$$\nabla^2 U(r,z,t) + 1/k_0 g(r,z,t) = 1/\alpha \frac{\partial}{\partial t} U(r,z,t), \quad (\text{A3})$$

where $\alpha = k(T)/\rho c$.

For the materials of interest in thermoluminescence dosimetry, the thermal diffusivity $\alpha = \alpha(T)$ varies very little with temperature and can be assumed constant. The initial and boundary conditions for Eq. (A3) can be derived from the original conditions⁹ using Eq. (A2) and the solution has the same form as Eq. (7a).

For the case of LiF,³⁵ the thermal conductivity may be fitted by a function of the form

$$k(T) = k_0 T_0 / T. \quad (\text{A4})$$

In our case, T_0 is the room temperature. Then the Kirchhoff transformation gives

$$U = T_0 \ln(T/T_0), \quad (\text{A5})$$

and the temperature expression in terms of U can be extracted from Eq. (A5) as

$$T(r,z,t) = T_0 \exp[U(r,z,t)/T_0], \quad (\text{A6})$$

where $U(r,z,t)$ is given as

$$U(r,z,t) = \frac{(1-R)\alpha P}{\pi k L} \int_{r=0}^r dt \frac{e^{-r^2[4\alpha t - \tau] + w^2}}{4\alpha(t-\tau) + w^2} \times \left[1 - e^{-\mu L} + 2 \sum_{m=1}^{\infty} \frac{e^{-\alpha m^2 r^2 t - \pi/L^2}}{1 + \left(\frac{m\pi}{\mu L}\right)^2} \right] \times (1 - \cos m\pi) \cos\left(\frac{m\pi z}{L}\right). \quad (\text{A7})$$

APPENDIX B

The parameter combination defining B in Eq. (9) of Sec. III B contains the thermal properties, the reflectivity, and the absorption coefficient for the TL sample as well as the power of the laser heating beam. In principle, these may be measured separately. However, that turns out to be rather difficult for the self-supporting thermoluminescent foils, because the material is a composite of a powder and a polymer. Therefore, we developed a method to determine B experimentally so as to be able to calculate the temperature distribution $T(r,z,t)$ and the resulting glow curves of these dosimeter configurations, whose total absorption of the laser heating beam is not too large (no dependence on z). It will be shown that it is possible to extract B from the incandescent background emission of the heated spot on the sample.

As described in Sec. III, incandescent emission from the center hot spot of a sample exposed to the Gaussian laser

beam is always present when TL glow curves are measured and the laser beam is not prematurely turned off [see Fig. 9(b)].

The energy density for a given wavelength λ of the incandescent blackbody emission is given by Planck's law:

$$U_\lambda = 8\pi hc\lambda^{-5} \left[\exp\left(\frac{hc}{\lambda kT}\right) - 1 \right]^{-1} \quad (\text{B1})$$

where T is the absolute temperature, and h and k have the usual meaning. We tried to keep the temperature below 600 K in order not to destroy the sample which visibly darkened by only briefly heating it above that limit. Therefore we can assume $hc/\lambda kT \ll 1$, and Eq. (B1) reduces to

$$U_\lambda = 8\pi hc\lambda^{-5} \exp\left(-\frac{hc}{\lambda kT}\right). \quad (\text{B2})$$

The total intensity I in the spectral range of sensitivity of the photomultiplier tube is given by

$$I_b \propto \int_{\lambda_1}^{\lambda_2} K(\lambda) U_\lambda d\lambda, \quad (\text{B3})$$

where $K(\lambda)$ is the quantum efficiency. It turned out to be a linearly decreasing function of the wavelength between 600 and 650 nm, the wavelength interval utilized in our experiments. This yields

$$I_b \propto \exp\left(-\frac{hc}{\bar{\lambda}kT}\right), \quad (\text{B4})$$

where $\bar{\lambda}$ is at the center of this sensitivity region which is determined by the photomultiplier and a short wavelength cutoff filter (see below).

In order to eliminate the unknown proportionality constant in Eq. (B4), one can utilize the ratio of the first derivative with respect to time and this expression. This ratio is readily determined experimentally:

$$\left(\frac{\partial I}{\partial t}\right)/I \propto (a/T^2) \exp(-a/T) (dT/dt) \quad (\text{B5})$$

and

$$\left(\frac{\partial I}{\partial t}\right)/I = (a/T^2) (dT/dt), \quad (\text{B6})$$

where $a = hc/\bar{\lambda}k$.

The time dependence of the temperature is given by Eq. (8) of Sec. III B. We may consider the simplest case which for the temperature is proportional to the time t . This is valid only for $4\alpha t < \omega^2$ and yields

$$T - T_0 \propto Bt/\omega^2. \quad (\text{B7})$$

Then

$$\left(\frac{\partial I}{\partial t}\right)/I = [a/(Bt/\omega^2 + T_0)^2] (B/\omega^2). \quad (\text{B8})$$

The quantity B is calculated by determining this ratio experimentally and careful measurement of the $1/e$ full width 2ω of the laser beam.

EXPERIMENT RESULTS

One of the four different dosimeter configurations was a polyimide film loaded with LiF powder. Both materials of this 84- μm -thick composite film absorb the 10.6- μm heating

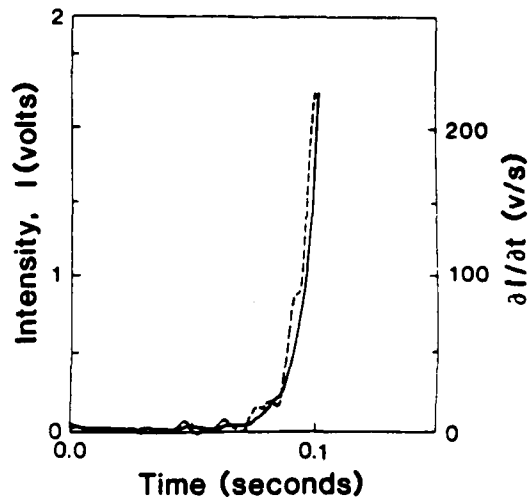


FIG. 16. Determination of $B = (1 - R)(1 - e^{-\alpha t})P/\pi\rho cL$ [see Eq. (9)] for powder-loaded Kapton foils by the incandescence method described in Appendix B. Shown are the rise of the incandescence emission I (solid line) and its time-derivative $(\partial I/\partial t)/I$ (dashed line) as a function of time after exposure of the foil (without previous exposure to ionizing radiation to eliminate thermoluminescent emission) to a 4.8-W laser beam of spot size $2\omega = 0.118$ cm ($\partial I/\partial t$). From the ratio $(\partial I/\partial t)/I$, determined between zero and 0.03 s, B was found to be 27 ± 3 K cm^2/s for this laser power.

photons only moderately. One can, therefore, assume that Eq. (8) is applicable.

The parameter combination B of Eq. (9) is straightforwardly determined by recording the time evolution of the incandescent emission at a narrow wavelength interval around $\bar{\lambda}$. Using a step filter having a low-wavelength transmission cutoff at 600 nm (interference filter type 6135-650, Optics Technology, Palo Alto, California). Together with an EMI 9924B PMT yielded $\bar{\lambda} = 625$ nm. The incandescent signal obtained by heating this foil with $P = 4.8$ W and $2 = 0.118$ cm is shown in Fig. 16 together with its derivative as obtained by digital processing with the Data Precision DP6000 waveform analyzer. From the ratio $(\partial I/\partial t)/I$, again calculated directly with the DP6000, B was determined to be $27 \text{ cm}^2 \text{ K/s}$ for the laser power stated above. The condition $4\alpha t < \omega^2$ is fulfilled with the values $\alpha = 0.0175 \text{ cm}^2/\text{s}$ (see Sec. III B), $t = 0.03$ sec, and $\omega = 0.059$ cm.

It should be pointed out that the above method is not applicable for the dosimeter configuration described in Sec. III, cases 1, 3, and 4 because here the z dependence of the temperature rise cannot be neglected and Eq. (8) is not valid.

¹J. Gasiot, P. Bräunlich, and J. P. Fillard, *J. Appl. Phys.* **53**, 5200 (1982).

²P. Bräunlich, J. Gasiot, J. P. Fillard, and M. Castagne, *Appl. Phys. Lett.* **39**, 769 (1981).

³P. Bräunlich, S. C. Jones, and W. Tetzlaff, *Radiat. Protection Dosimetry* **6**, 103 (1984).

⁴P. Kelly, P. Bräunlich, A. Abtahi, S. C. Jones, and M. deMurcia, *Radiat. Protection Dosimetry* **6**, 25 (1984).

⁵P. Bräunlich, W. Tetzlaff, J. Gasiot, and S. C. Jones, *Proceedings of the International Beta Dosimetry Symposium*, Washington, D.C. (1983), U.S. Nuclear Regulatory Commission Publication No. NUREG/CP-0050, p. 293 (available from National Technical Information Center, Springfield, VA 22161).

- ⁹P. Bräunlich, M. Brown, J. Gasiot, and J. P. Fillard, Proceedings of the Ninth DOE Workshop on Personnel Neutron Dosimetry, Las Vegas (1982), U.S. Department of Energy Publication No. CONF-820668, p. 193 (available from the Battelle Pacific Northwest Laboratories, Richland, WA 99352 as Report no. PNL-SA-10714).
- ⁷V. K. Mathur, M. D. Brown, and P. Bräunlich, *Radiat. Protection Dosimetry* **6**, 163 (1984).
- ⁸Y. Yasuno, H. Tsutsui, O. Yamamoto, and T. Yamashita, *Jpn. J. Appl. Phys.* **21**, 967 (1982).
- ⁹P. Bräunlich, S. C. Jones, A. Abtahi, and M. deMurcia, *Radiat. Protection Dosimetry* **6**, 83 (1984).
- ¹⁰C. Han, Y. Ishi, and Murata, *Appl. Opt.* **22**, 3644 (1983).
- ¹¹Harshaw Chemical Co., 6801 Cochran Road, Solon, OH 44139.
- ¹²G. Portal, "Preparation and Properties of Principal TL Products," in *Applied Thermoluminescence Dosimetry*, edited by M. Oberhofer and A. Scharmann (Adams Hilger, Bristol, 1980), pp. 97-122.
- ¹³P. Bräunlich and W. Tetzlaff (unpublished).
- ¹⁴M. Sparks, *J. Appl. Phys.* **47**, 837 (1976).
- ¹⁵P. Bräunlich, Final Report, "Development of Laser Heating Techniques in Beta Thermoluminescence Dosimetry," Jan. 1984, prepared for the Pacific Northwest Laboratories, Battelle Memorial Institute, Subcontract no. B-81227-A-X (unpublished).
- ¹⁶P. Bräunlich, P. Kelly, and J. P. Fillard, "Thermally Stimulated Luminescence and Conductivity," in *Thermally Stimulated Relaxation in Solids*, edited by P. Bräunlich (Springer, Berlin, 1979).
- ¹⁷P. Kelly, M. Laubitz, and P. Bräunlich, *Phys. Rev.* **84**, 1960 (1971).
- ¹⁸W. Shockley and W. T. Read, Jr., *Phys. Rev.* **87**, 835 (1952).
- ¹⁹P. Bräunlich, "Introduction and Basic Principles," in *Thermally Stimulated Relaxation in Solids* (Springer, Berlin, 1979).
- ²⁰S. W. S. McKeever, *Nuc. Instrum. Methods* **175**, 19 (1980).
- ²¹N. Vana and G. Ritzinger, *Radiat. Protection Dosimetry* **6**, 29 (1984).
- ²²A. B. Donaldson, *J. Franklin Inst.* **294**, 275 (1972).
- ²³Y. I. Nissim, A. Lietoila, R. B. Gold, and J. F. Gibbons, *J. Appl. Phys.* **51**, 274 (1980).
- ²⁴J. R. Meyer, M. R. Kruer, and F. J. Bartoli, *J. Appl. Phys.* **51**, 5513 (1980).
- ²⁵J. R. Meyer, F. J. Bartoli, and M. R. Kruer, *Phys. Rev. B* **21**, 1559 (1980).
- ²⁶A. Maruani, Y. I. Nissim, F. Bonnouvrier, and D. Paquet, *Proceedings of the Symposium on Laser Solid State Interactions and Transient Thermal Proceedings of Materials*, Mater. Res. Soc. Symp. Proc. **13**, 123 (1983).
- ²⁷A. Maruani, Y. I. Nissim, F. Bonnouvrier, and D. Paquet, *J. Phys. (Paris) Colloq.* **CS**, 87 (1983).
- ²⁸E. Bernal G., *Appl. Opt.* **14**, 314 (1975).
- ²⁹M. Sparks, *J. Appl. Phys.* **47**, 837 (1976).
- ³⁰R. E. Warren and M. Sparks, *J. Appl. Phys.* **50**, 7952 (1979).
- ³¹H. S. Carslaw and J. C. Jaeger, *Conduction of Heat in Solids*, 2nd ed. (Oxford University, Oxford, 1959), p. 112.
- ³²M. N. Ozisik, *Heat Conduction* (Wiley, New York, 1980).
- ³³G. Brost, P. Horn, and A. Abtahi, *Appl. Opt.* **24**, 38 (1985).
- ³⁴A. H. Firester, M. E. Heller, and P. Sheng, *Appl. Opt.* **16**, 197 (1977).
- ³⁵A. V. Petrov, N. S. Tsytkina, and V. E. Seleznev, *High Temperatures-High Pressures* **8**, 537 (1976).

Abdollah Abtahi and Peter F. Braunlich

Department of Physics, Washington State University, Pullman, Washington 99164-2814

Paul Kelly

Division of Physics, National Research Council, Ottawa, Canada, K1A 0R6

(Received 19 May 1986; accepted for publication 28 July 1986)

A general solution of the heat diffusion equation is presented for the case of a semi-infinite two-layer system that is heated with a localized cw laser beam of Gaussian or uniform circular intensity profile. As an example, this theory is applied to thin layers of a thermoluminescent material on glass substrates. The transient thermoluminescence emission response is calculated and compared with experimental results, illustrating the validity of the solutions. Applications to transient laser heating of oxide-semiconductor sandwiches are discussed.

I. INTRODUCTION

The interest in heating semi-infinite slabs with localized laser beams stems from the application of laser heating in thermoluminescence dosimetry, which recently has received considerable attention.¹⁻⁵ The early work in this field was restricted to the use of cw CO₂ laser beams having Gaussian intensity profiles. The theoretical approach taken for the calculations of the thermoluminescence (TL) response of a thin TL layer on a glass substrate assumed that the TL layer thickness is negligibly small compared to that of the substrate. All thermal properties of the sample were assumed to be due to the substrate alone. Only the reflectivity and absorptance, due to modification of the glass substrate by the thin TL layer, were taken into account. The agreement between experimental TL responses and calculated ones was satisfactory for a number of layer configurations consisting of LiF:Mg, Ti powder (Harshaw/Filtrol TLD-100) on borosilicate glass.⁵

For practical applications of laser stimulated thermoluminescence in dosimetry it became apparent, however, that Gaussian beam profiles impose unnecessary restrictions.⁶ We have, therefore, developed the optical technology to produce spatially uniform beam intensity profiles,⁷ which was modified for uniform circular beams, and we subsequently attempted to calculate the thermoluminescence response functions obtained with such a beam on the basis of the simple one-layer theory presented in Ref. 5. It turned out that this theory did not yield the characteristic TL glow curves measured under these conditions. This failure prompted us to work out the theory of localized laser beam heating of a two-layer system. It is the purpose of the present paper to present the general solutions of the heat diffusion equation for this case and apply the theory to the same type of thin-layer thermoluminescence dosimetry configuration (LiF:Mg, Ti TL powder on a borosilicate glass substrate) used for the work described in Ref. 5. For completeness, we have also recalculated the transient heating and the resulting TL response of this two-layer configuration for Gaussian heating beams. It is perhaps worthwhile to point out that the solutions described in this paper are of general validity and

may well be useful in other fields of endeavor; i.e., laser annealing of semiconductors.

II. SOLUTIONS TO THE HEAT EQUATIONS

The system we consider consists of two layers of material in perfect thermal contact. As an example, picture again a thin layer of a thermoluminescent phosphor on a glass substrate or an oxide layer on a semiconductor. Each layer is characterized by its absorption coefficient for the laser photons μ_i , thermal conductivity k_i , thermal diffusivity α_i , and thickness l_i . The index $i = 1, 2$ denotes the respective layer and the total thickness is $L = l_1 + l_2$. We also assume that the laser beam impinges along the z axis perpendicularly to the x, y plane of the two-layer configuration. The laser beam profile is either circular and uniform (Fig. 1) or Gaussian.

The thermal diffusion equation in cylindrical coordinates (ignoring the effect of the finite speed of heat propagation⁸) is given by

$$\frac{r^{-1} \partial [rk_i \partial T_i(r, z, t) / \partial r]}{\partial r} + \frac{\partial [k_i \partial T_i(r, z, t) / \partial z]}{\partial z} + g_i(r, z, t) = \left(\frac{k_i}{\alpha_i} \right) \frac{\partial T_i(r, z, t)}{\partial t} \quad (1)$$

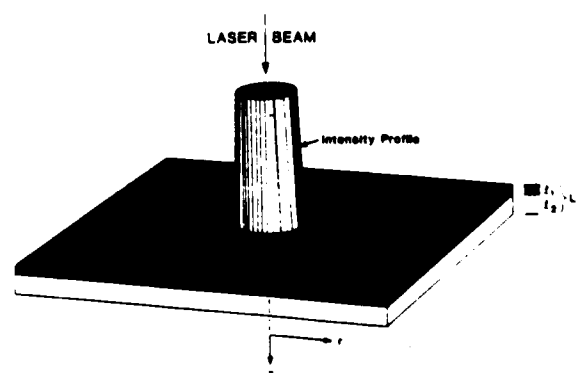


FIG. 1. Schematic representation of a uniform circular beam profile impinging on the surface at $z = 0$ of a two layer system of total thickness L .

We solve it for the following boundary conditions:

(1) The two-layer slab is infinite in radial direction and $T_i(r, z, t) \rightarrow T_0$ as $r \rightarrow \infty$;

(2) no heat loss occurs at the boundaries; i.e., $\partial T_i / \partial z = 0$ at $z = 0$ ($i = 1$) and $z = L$ ($i = 2$);

(3) at the interface ($z = l_1$), $T_1 = T_2$ and $k_1 \partial T_1 / \partial z = k_2 \partial T_2 / \partial z$.

The initial conditions are $T_i(r, z, t) = T_0$; i.e., room temperature, when the laser is turned on at $t = 0$. The temperature $T_i(r, z, t)$, obtained from Eq. (1), is the actual temperature increase above T_0 . Let $\Delta T_i(r, z, t) = T_i(r, z, t) - T_0$.

Correcting for reflection loss at the front surface at $z = 0$, the source functions become for $0 < t \leq t_p$ (t_p is the laser pulse duration)

$$g_1(r, z, t) = \mu_1(1 - R_1)(P^*/\pi\omega^2)\exp(-\mu_1 z)f(r, \omega) \quad (2)$$

and

$$g_2(r, z, t) = \mu_2(1 - R_1)(1 - R_2)(P^*/\pi\omega^2) \times \exp[-\mu_1 l_1 - \mu_2(z - l_1)]f(r, \omega), \quad (3)$$

where $f(r, \omega) = H(\omega - r)$ for the uniform beam and $f(r, \omega) = \exp(-r^2/\omega^2)$ for the Gaussian beam. P^* is the total laser power (not the power density) incident on the front surface, H the Heaviside step function, R_i the reflectivity of layer i , and ω the radius of the uniform circular beam or the $1/e$ half-width for the Gaussian beam.

We solve Eq. (1) with the initial and boundary conditions given above by the Green's function technique.⁹ The general solution, written compactly, is then

$$\Delta T_i(r, z, t) = \int_0^t d\tau \int_0^\infty r' dr' \left(\frac{\alpha_1}{k_1} \times \int_0^{l_1} dz' G_{i1}(r, z, t/r', z', \tau) g_1(r', z', \tau) + \frac{\alpha_2}{k_2} \int_{l_1}^L dz' G_{i2}(r, z, t/r', z', \tau) g_2(r', z', \tau) \right), \quad (4)$$

$$G_{ij} = \frac{k_j}{\alpha_j} \int_0^\infty \frac{\gamma_i d\gamma_i}{\alpha_i} \exp[-(\gamma_i^2 + \eta_i^2)(t - \tau)] \times J_0\left(\frac{\gamma_i r}{\sqrt{\alpha_i}}\right) J_0\left(\frac{\gamma_i r'}{\sqrt{\alpha_j}}\right) \frac{[x_i(z)x_j(z')]}{N}, \quad (5)$$

$$N = \sum_{i=1}^2 \frac{k_i l_i}{2\alpha_i} \frac{[1 + \sin(2\theta_i)/2\theta_i]}{\cos^2(\theta_i)},$$

$$\text{where } \theta_i = \xi_i l_i / \sqrt{\alpha_i}, \quad (6)$$

$$x_i(z) = \begin{cases} \cos(\xi_i z / \sqrt{\alpha_i}) / \cos(\xi_i l_1 / \sqrt{\alpha_1}) & \text{for } i = 1 \\ \cos[\xi_i(L - z) / \sqrt{\alpha_2}] / \cos(\xi_i l_2 / \sqrt{\alpha_2}) & \text{for } i = 2. \end{cases} \quad (7)$$

From the boundary conditions at the interface we have

$$\gamma_1 / \sqrt{\alpha_1} = \gamma_2 / \sqrt{\alpha_2} = \beta, \quad (8)$$

$$\sum_{i=1}^2 \frac{k_i \xi_i}{\sqrt{\alpha_i}} \tan\left(\frac{\xi_i l_i}{\sqrt{\alpha_i}}\right) = 0, \quad (9)$$

and

$$\xi_2^2 = \xi_1^2 + \beta^2(\alpha_1 - \alpha_2). \quad (10)$$

The rise in temperature then becomes

$$\Delta T_i(r, z, t) = [(1 - R_1)P^*/\pi\omega^2 N] \int_0^t d\tau \int_0^\infty r' dr' \int_0^\infty \beta d\beta \exp[\alpha_i \beta^2(t - \tau)] J_0(\beta r) \times J_0(\beta r') f(r', \omega) x_i(z) \exp[-\xi_i^2(t - \tau)] \{ \mu_1^2 \exp(-\mu_1 l_1) \times [\exp(\mu_1 l_1) + (\xi_1 / \mu_1 \sqrt{\alpha_1}) \sin(\xi_1 l_1 / \sqrt{\alpha_1}) - \cos(\xi_1 l_1 / \sqrt{\alpha_1})] / [(\mu_1^2 + \xi_1^2 / \alpha_1) \cos(\xi_1 l_1 / \sqrt{\alpha_1})] + (1 - R_2) \mu_2^2 \times \exp(-\mu_2 l_2) [\cos(\xi_2 l_2 / \sqrt{\alpha_2}) + (\xi_2 / \mu_2 \sqrt{\alpha_2}) \sin(\xi_2 l_2 / \sqrt{\alpha_2}) - \exp(-\mu_2 l_2)] / [(\mu_2^2 + \xi_2^2 / \alpha_2) \cos(\xi_2 l_2 / \sqrt{\alpha_2})] \}. \quad (11)$$

This general solution can be simplified for all those two-layer structures for which one of the layers is much thinner than the other one, which should be valid for the case of laser annealing. As we will show below in several examples, the spatio-temporal temperature distribution of such a configuration can be calculated by assuming $\alpha_1 = \alpha_2 = \alpha$. This assumption entails that the general form of the solution is maintained in regards to the deposition of the laser photons according to the absorption coefficients μ_1 and μ_2 , however, thermal diffusion is governed mainly by the thicker one of the two layers. Lateral heat diffusion in the thinner of the two layers is negligible. Instead, lateral heating occurs via diffusion in the thicker layer with heat transport across the interface into the thinner layer. For this case, the integration over β and r' in Eq. (11) is readily carried out, yielding

$$\Delta T_i(r, z, t) = \frac{BP^*}{\omega^2} \int_0^t d\tau Q(r, t - \tau) \left(1 + \frac{1 - R_1}{\pi B} \sum_{m=1}^{\infty} \exp(-\mu_1 l_1) [\exp(\mu_1 l_1) - \cos(\eta_m l_1) + (\eta_m / \mu_1) \sin(\eta_m l_1)] \right) \times [N_m(1 + \eta_m^2 / \mu_1^2) \cos(\eta_m l_1)] + (1 - R_2) \exp(-\mu_2 l_2) \times [\cos(\eta_m l_2) + (\eta_m / \mu_2) \sin(\eta_m l_2) - \exp(-\mu_2 l_2)] / [N_m(1 + \eta_m^2 / \mu_2^2) \cos(\eta_m l_2)] x_i(z) \exp[-\alpha \eta_m^2(t - \tau)], \quad (12)$$

with $Q(r,t) = P(\omega/\sqrt{2\alpha t}, r/\sqrt{2\alpha t})$ for uniform circular beam or $\exp[r^2/(\omega^2 + 4\alpha t)]/(1 + 4\alpha t/\omega^2)$ for Gaussian beam profile, where

$$P(\omega, r) = \int_0^\omega \omega' d\omega' I_0(\omega', r) \exp[-(\omega'^2 + r^2)/2]$$

is called the circular coverage function¹⁰ or the "p" function.¹¹

$$\xi_1/\sqrt{\alpha_1} = \xi_2/\sqrt{\alpha_2} = \eta_m,$$

$$B = (1 - R_1) [1 - (1 - R_2) \exp(-\mu_1 l_1 - \mu_2 l_2) - R_2 \exp(-\mu_1 l_1)] / \pi N_0,$$

and, from the boundary conditions, the transcendental equation

$$k_1 \tan(\eta_m l_1) + k_2 \tan(\eta_m l_2) = 0, \quad (13)$$

where the roots η_m , $m = 1, 2, \dots$, are derived in the Appendix.

We illustrate the validity of these results obtained for both the uniform circular and the Gaussian beam by monitoring the thermoluminescence response of a thin TL layer on a glass substrate. We choose as an example a 35–40- μm -thick LiF:Mg, Ti layer on a 150- μm -thick borosilicate micro-

scope cover slide. The transient temperature distribution is indirectly monitored via the transient thermoluminescence response of the thin active layer to localized laser heating, measured with a photomultiplier. We point out, however, that in this way the spatially integrated TL signal is measured without spatial resolution. Only the temporal evolution of the thermoluminescence signal is monitored. The procedure for calculating the thermoluminescence transient is based on the well-known electron kinetics for this thermoluminescent phosphor (see below).

The absorption coefficient of LiF for 10.6- μm CO₂ laser photons is 40 cm⁻¹, while that of glass is much higher ($\sim 10^4$ cm⁻¹). Consequently, we have $\mu_1 l_1 \ll 1$ for the LiF layer and $\mu_2 l_2 \gg 1$ for the glass substrate. We have locally heated this structure with laser beams of Gaussian and uniform circular profiles, constant power P^* , and various beam sizes from both sides, that is the active TL layer can either be on top at $z = 0$ or at the bottom at $z = L$, and we have monitored the transient thermoluminescence response in both cases. The transient temperature distributions are readily obtained from Eq. (12) as follows.

Case 1. Thermoluminescent layer on top of the glass substrate ($\mu_1 l_1 \ll 1$).

$$\Delta T_1(r, z, t) = (BP^*/\omega^2) \int_0^t d\tau Q(r, t - \tau) \left(1 + N_0 \sum_{m=1}^{\infty} \cos(\eta_m z) \exp[-\alpha \eta_m^2 (t - \tau)] / [N_m (1 + \eta_m^2 / \mu_2^2) \cos(\eta_m l_1)] \right). \quad (14)$$

Case 2. Thermoluminescent layer at the bottom of the glass substrate ($\mu_2 l_2 \ll 1$).

$$\Delta T_2(r, z, t) = (BP^*/\omega^2) \int_0^t d\tau Q(r, t - \tau) \left(1 + N_0 \sum_{m=1}^{\infty} \cos[\eta_m (L - z)] \exp[-\alpha \eta_m^2 (t - \tau)] / [N_m (1 + \eta_m^2 / \mu_1^2) \cos(\eta_m l_1) \cos(\eta_m l_2)] \right). \quad (15)$$

In Eqs. (12) and (15), we have written $N_0 = (1/\alpha) \sum_{i=1}^2 k_i l_i$ and

$$N_m = (1/2\alpha) \sum_{i=1}^2 k_i l_i [1 + (\sin 2\theta_i)/(2\theta_i)] / \cos^2 \theta_i,$$

where $\theta_i = \eta_m l_i$. The calculations were performed with the following values for the thermal conductivities of the two layers in Case 1 (reverse in Case 2):

- (1) TL layer: $k_1 = 0.0275$ W/K cm.
- (2) Glass substrate: $k_2 = 0.00942$ W/K cm.

Both of these values are temperature dependent. The temperature dependence of k_2 for glass is given by $k_2 = 0.00942 (1 + \sigma \Delta T_2)$ with $\sigma = 0.00222$ K⁻¹.¹² This can be accounted for in our calculations by the method of the Kirchhoff transformation.⁵ A "corrected temperature"

$$T_{N_2} = T_0 + \sigma^{-1} [(1 + 2\sigma \Delta T_2)^{1/2} - 1]$$

is introduced with the same σ . The temperature dependence of k_1 for LiF does not have to be accounted for since it is the very thin layer and, as we explained above, lateral heat diffusion is dominated by the thicker glass layer.

The thermal diffusivity, α , assumed to be identical for both layers (see above), requires special attention. Accord-

ing to the glass manufacturer,¹² it is slightly temperature dependent as well. It varies from 0.0052 to 0.0057 cm²/s between 0 and 100 °C, respectively, and it is expected to be somewhat higher at the highest temperature of 400 °C reached in our measurements. We choose not to correct for this small variation in α with T . Instead, we determine an average value for the thermal diffusivity by the best fit of the calculate and the measured thermoluminescence response curves obtained with the uniform circular beam. It turns out that the high temperature decay of this curve is very sensitive to slight variations in α . The best fit to the shape in all cases reported on below (including the ones where a Gaussian beam was employed) was obtained with $\alpha = 0.0064$ cm²/s. This value is consistent with expectation as the peak of the TL response curve occurs at about 250 °C, which appears to be a good "average" temperature for which to select a value for the thermal diffusivity.

For computational efficiency, the numerical calculations of Eqs. (14) and (15) start at the lower time limit of $t = 10^{-6}$ s rather than zero. This can be done since, for laser powers that are believed to be practical in thermoluminescence dosimetry applications, the temperature rise any-

where in the sample during the initial microsecond is always much smaller than the temperature at which any thermoluminescence signal can be detected.

The prefactor $B = (1 - R_1)(1 - R_2)/\pi N_0$ in Eqs. (14) and (15) is given by the optical and thermal properties of the two-layer sample, but it cannot be easily calculated because of the inhomogeneity of the TL powder layer. Therefore, we measure it by the procedure described in Ref. 5. This procedure determines the absorbance and B is, except for a constant factor, the fraction of the laser power absorbed by the two-layer system. Its measurement automatically includes the reflection on the front surface and the interface. However, the accuracy of these experiments is only about $\pm 25\%$. For calculation of TL responses, a value within this error is chosen to fit experimental data. The roots obtained from the boundary condition are derived in the Appendix.

The thermoluminescence glow curves we consider are commonly called peaks 3, 4, and 5. They are sufficiently well described by simple first-order kinetics with attempt-to-escape frequencies of $4 \times 10^{13} \text{ s}^{-1}$, $7.3 \times 10^{15} \text{ s}^{-1}$, and $4 \times 10^{21} \text{ s}^{-1}$, and trap depths of 1.23, 1.54, and 2.17 eV, respectively.¹³ Their relative intensities are adjusted to yield the actual glow curve measured with conventional uniform heating. Peaks 1 and 2 are removed by a 10-min pre-anneal treatment at 100 °C. The two-layer configuration is irradiated with ⁶⁰Co γ rays to fill the electron traps and exposed to a uniform circular CO₂ laser beam of fixed 6.5 W power both from the front (active TL layer exposed directly) and from the back (active layer heated via diffusion through the glass substrate, which is exposed to the laser beam). Laser heating generates a time-dependent transient spatial temperature distribution which results in the TL emission response shown in Figs. 2(a) and 2(b), measured without spatial resolution by a photomultiplier detector. As stated above, the one-layer theory does not yield satisfactory agreement with measured thermoluminescence response curves when the heating beam has a uniform circular intensity profile. These curves have a pronounced peak; however, due to lateral diffusion, the thermoluminescence intensity does not vanish completely, when heating is continued much longer after peak occurrence. The simple two-layer theory, Eqs. (14) and (15), calculated both with and without the temperature dependence of the thermal conductivity taken into account via the Kirchhoff transformation technique, is compared with the experimental results obtained for a fixed laser power of 6.5 W and a beam radius of $\omega = 0.15 \text{ cm}$ [Figs. 2(a) and 2(b)]. The thermal diffusivity chosen was again $\alpha = 0.0064 \text{ cm}^2/\text{s}$ (an "average temperature value"). The prefactor B was selected to yield the best fit of the peak location. It is to be compared with experimental values, determined with the method of Ref. 5, for both front and back heating of $B = 10.7 \pm 25\% \text{ K cm}^2/\text{J}$ and $B = 6.3 \pm 20\% \text{ K cm}^2/\text{J}$, respectively. The agreement between the measured and the calculated thermoluminescence response curves is very good, confirming the validity of the theoretical approach presented above.

We have carried out a detailed program exploring the thermoluminescence response curves obtained under var-

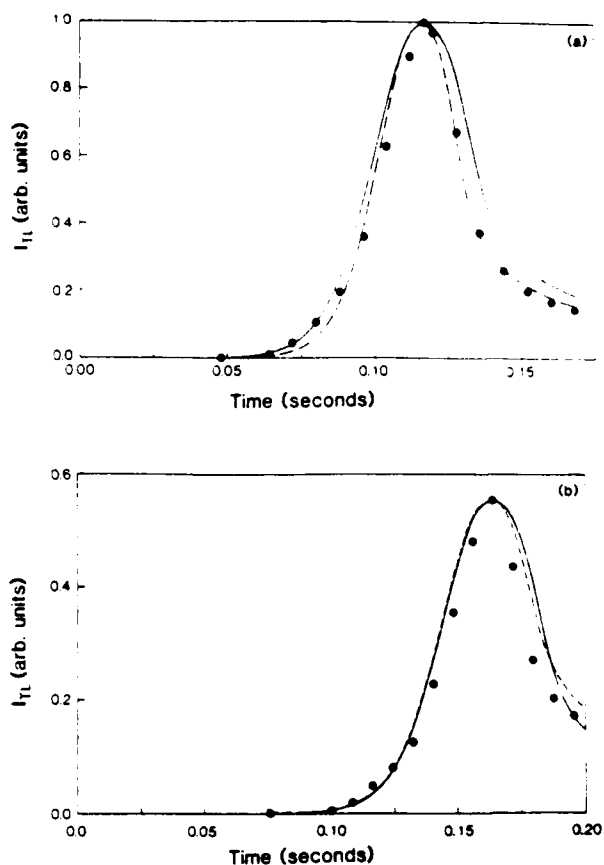


FIG. 2. (a) TL response curve measured with a 6.5-W CO₂ laser beam ($\omega = 0.15 \text{ cm}$ for the uniform circular beam profile) by heating the phosphor coating on top of a glass substrate. The dashed curve is obtained with $B = 7.55 \text{ K cm}^2/\text{J}$, $\alpha = 0.0064 \text{ cm}^2/\text{s}$, using Eq. (14) of the text. The full curve is the fit obtained with $B = 9.4 \text{ K cm}^2/\text{J}$, the same α , and the Kirchhoff transformation. (b) TL response when the laser beam impinges onto the side opposite to the phosphor coating. The dashed curve is the fit obtained with $B = 6.0 \text{ K cm}^2/\text{J}$ at 6.5-W laser power, $\alpha = 0.0064 \text{ cm}^2/\text{s}$, using Eq. (15) of the text. The solid line is the fit obtained with $B = 10 \text{ K cm}^2/\text{J}$, the same α , and the Kirchhoff transformation.

ious experimental conditions for the purpose of characterizing this type of laser heating in dosimetry applications. The results will be presented in a forthcoming publication.^{14,15}

Figures 3(a) and 3(b) are families of curves measured for different $1/e$ widths ω of the Gaussian laser beam. The previous one-layer approximation⁵ yielded a satisfactory fit only by adjusting the prefactor B . With the two-layer heat equation, we obtain the curves drawn through the experimental points in Figs. 3(a) and 3(b) in one case, without correcting for the temperature dependence of the thermal conductivity and, for comparison, when the temperature dependence is taken into account by the method of the Kirchhoff transformation as described above. Again, the prefactor B had to be adjusted slightly for fit. We note that the two-layer theory represents a rather marked improvement of the previous one-layer approximation.

In conclusion, we have presented a general theory of heating two-layer systems with localized laser beams of Gaussian and uniform circular intensity profiles, and

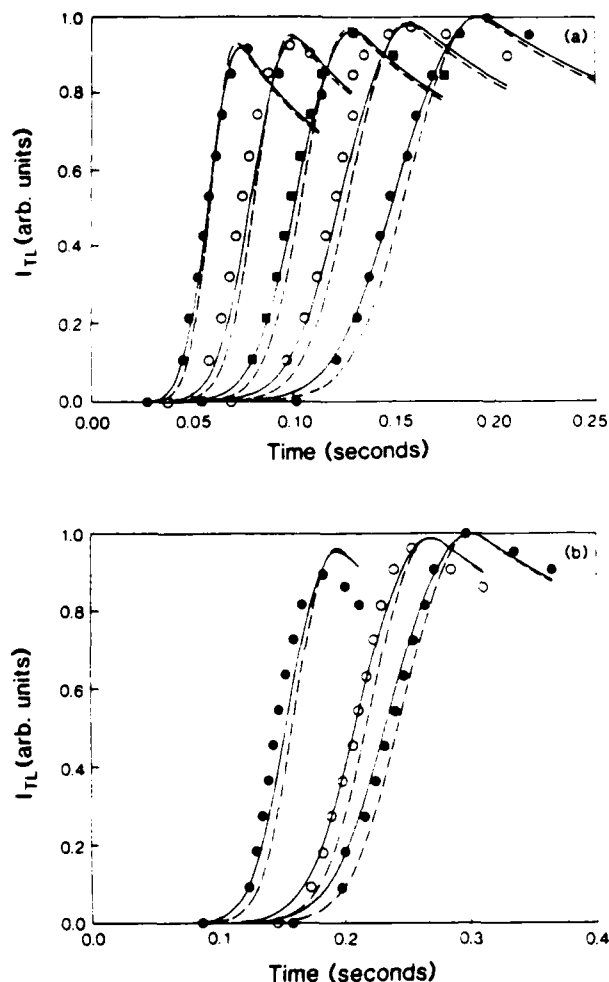


FIG. 3. (a) TL response curves from Fig. 12, Ref. 5 recalculated using a 4.45-W CO₂ laser beam with a Gaussian intensity profile by heating the phosphor-coated side on a glass substrate. The families of curves are the fit obtained with $B = 5.17 \text{ K cm}^2/\text{J}$ with the Kirchhoff transformation (solid lines) and $B = 4.05 \text{ K cm}^2/\text{J}$ without the Kirchhoff transformation (dashed lines) using $\alpha = 0.0064 \text{ cm}^2/\text{s}$, the same as Fig. 2 for the following full widths at $1/e$ of the peak intensity of the laser beam 2ω (mm): 2.03, 1.83, 1.65, 1.45, and 1.24 (curves from left to right, respectively). (b) TL response curves from Fig. 13 Ref. 5 recomputed with a 4.18-W Gaussian laser beam by heating TL coating through the glass substrate. The dashed curves are obtained with $B = 3.35 \text{ K cm}^2/\text{J}$ and the solid lines are curves obtained with $B = 4.3 \text{ K cm}^2/\text{J}$, using the Kirchhoff transformation and $\alpha = 0.0064 \text{ cm}^2/\text{s}$ for the following measured beam widths 2ω (mm): 2.13, 1.994, and 1.65 (curves from left to right, respectively).

checked its validity by comparing calculated and measured thermoluminescence response curves obtained with thin-layer TL phosphor layer on glass substrates. The theory is well suited for all systems that consist of a layer of a given material in perfect contact with a substrate of different optical and thermal properties. In particular, we expect the theory described in Eqs. (1)–(11) to be applicable to local heating (laser annealing) of thin oxide or epitaxial layers on semiconductor or insulator substrates.

ACKNOWLEDGMENT

This work was sponsored by the Office of Naval Research under Contract No. N00014-82-K-0529.

APPENDIX: CALCULATION OF PARAMETER η_m

In this work we have a poorly absorbing phosphor coating $l_1 = 0.2 L$ on a highly absorbing glass slide, $l_2 = 0.8 L$ where the total thickness $L = 0.01875 \text{ cm}$. In this case, m distinct roots η_m can be obtained from the transcendental equation $k_1 \tan(\theta) + k_2 \tan(4\theta) = 0$ with $\theta = 0.2\eta_m L$. With $F = 5\pi/L$, $h = 3 + 2/k$, $k = k_1/k_2$, $D^- = \{h + [h^2 - (1 + 4/k)]^{1/2}\}^{1/2}$, and $D^+ = \{h - [h + (1 + 4/k)]^{1/2}\}^{1/2}$, the m roots greater than $\eta_0 = 0$ are then given by

$$\eta_m = [\pi^{-1} \tan^{-1}(D^-) + (m-1)/5]F$$

for $m = 1, 6, 11, \dots$

$$= [\pi^{-1} \tan^{-1}(D^+) + (m-2)/5]F$$

for $m = 2, 7, 12, \dots$

$$= [1 - \pi^{-1} \tan^{-1}(D^+) + (m-3)/5]F$$

for $m = 3, 8, 13, \dots$

$$= [1 - \pi^{-1} \tan^{-1}(D^-) + (m-4)/5]F^2$$

for $m = 4, 9, 14, \dots$

$$= mF/5$$

for $m = 5, 10, 15, \dots$

The root $\eta_0 = 0$ yields the first term, unity, in the brackets of Eq. (12).

¹P. Braunlich, J. Gasiot, P. J. Fillard, and M. Castagné, *Appl. Phys. Lett.* **39**, 769 (1981).

²J. Gasiot, P. Braunlich, and J. P. Fillard, *J. Appl. Phys.* **53**, 5200 (1982).

³P. Braunlich, S. C. Jones, A. Abtahi, M. deMurcia, and P. Kelly, *Radiat. Prot. Dosimetry* **6**, 83 (1984).

⁴P. Braunlich, W. Tetzlaff, J. Gasiot, and S. C. Jones, *Proceedings of the International Beta Dosimetry Symposium*, Washington, D.C. (1983), U. S. Nuclear Regulatory Commission Publication, Report No. NUREG/CP-0050, p. 293 (Available from National Technical Center, Springfield, VA 22161).

⁵A. Abtahi, P. Braunlich, P. Kelly, *J. Appl. Phys.* **58**, 1626 (1985).

⁶W. Tetzlaff, P. Braunlich, and K. Swinth, *Proceedings of the DOE workshop on Beta Measurement*, Albuquerque, NM, Jan. 23–24, 1986 (to be published).

⁷P. Braunlich and W. Tetzlaff, Patent Pending, Serial No. 652,829 Case No. US-5 (1985).

⁸J. I. Frankel, B. Vick, and M. N. Ozisik, *J. Appl. Phys.* **58**, 3340 (1985).

⁹M. N. Ozisik, *Heat Conduction* (Wiley, New York, 1980).

¹⁰H. H. Germond, The Rand Corp., 1700 Main Street, Santa Monica, CA, RM-330 (1950).

¹¹J. I. Masters, *J. Chem. Phys.* **23**, 1865 (1955).

¹²Erie Scientific, Division of Syborn Corp., Portsmouth Industrial Park, Portsmouth, New Hampshire 03801.

¹³S. W. S. McKeever, *Nucl. Instrum. Methods* **175**, 19 (1980).

¹⁴P. Kelly, A. Abtahi, and P. Braunlich, *J. Appl. Phys.* (to be published).

¹⁵A. Abtahi, Ph.D. dissertation, Washington State University, May 1986.

Laser-stimulated thermoluminescence. II

Paul Kelly

Division of Physics, National Research Council, Ottawa, Canada K1A 0R6

Abdollah Abtahi and Peter F. Braunlich

Department of Physics, Washington State University, Pullman, Washington 99164-2814

(Received 11 July 1986; accepted for publication 12 September 1986)

The theory of heating a semi-infinite two-layer system with a localized CO₂ laser beam of uniform circular intensity profile is applied to configurations consisting of thin thermoluminescent LiF:Mg,Ti phosphor layers on borosilicate glass substrates. We study thermoluminescence because it serves as a convenient monitor for the temperature distribution and because of its importance in developing the laser-heating technique for solid-state dosimetry. Experimental and calculated results are compared in an attempt to completely characterize the thermoluminescence response curves. The two-layer system is heated in two different modes: the laser beam impinges onto (a) the phosphor layer, and (b) the glass substrate. We investigate in detail changes in the thermoluminescence response due to different laser powers and variations in the optical and thermal properties of the samples.

I. INTRODUCTION

In a previous publication¹ computational methods were presented for the characterization of the thermoluminescence (TL) response obtained from thin semi-infinite thermoluminescent phosphor layers on transparent substrates upon exposure to localized Gaussian laser beams. These luminescence responses (the thermoluminescence intensity measured without spatial resolution) are not the familiar TL glow curves,² but rather exhibit a complex shape with limited glow peak separation, which is the result of the nonuniform laser beam profile and the resulting nonuniform temperature distribution in the sample. At any given time after onset of laser exposure, the lateral temperature distribution is nearly Gaussian as well, modified somewhat by thermal diffusion. The spatially resolved TL emission from the thin layer resembles such a Gaussian distribution up to times nearly 2.5 times longer than the appearance of the peak of the spatially unresolved TL response curve.³ This curve typically exhibits a fast rise and a shallow peak, but never decays completely because of lateral heat diffusion.¹ The TL signal disappears only when the laser is turned off.

Nevertheless, laser heating of thin-layer thermoluminescent dosimeter configurations with focused Gaussian beams has been applied successfully to TL imaging⁴ and to rapid measurement of dose distributions generated by exposure to β rays behind attenuating filters of various thicknesses.⁵

For accurate and sensitive personnel and environmental thermoluminescence dosimetry, heating with a laser beam of uniform intensity profile is highly desirable. As we will demonstrate below, localized laser exposure of a semi-infinite phosphor layer on a substrate produces glow curves which are, except for a slowly decreasing tail on the high-temperature side of the peak, nearly identical to the ones obtained with conventional uniform heating.

In this paper we describe a TL laser heating apparatus that features a circular beam of uniform intensity profile

generated with a technique reported in Refs. 6 and 7. It was employed to study the thermoluminescence response curves from thin-layer LiF:Mg,Ti dosimeters on glass substrates under a variety of experimental conditions. The motivation for this investigation was, however, not limited to the establishment of the operating conditions for efficient and economical laser heating in thermoluminescence dosimetry and imaging (the latter with greatly improved spatial resolution as compared to the nonuniform Gaussian beam). We also felt that the thermoluminescence emission from a thin layer on a substrate is a very convenient monitor for the time evolution of the temperature distribution established in the two-layer system during localized heating with a laser beam of uniform intensity profile. The general theory of the heat transfer from such a beam to a semi-infinite two-layer system and the subsequent temperature diffusion was presented previously.^{3,8} In the following we will first briefly review the basic aspects of this theory, describe the experimental facility in some detail, and finally present experimental and computation results.

II. COMPUTATIONAL APPROACH

In applying the theory of Ref. 8 to a special system that consists of a thin thermoluminescent phosphor layer on a strongly absorbing substrate, a number of approximations can be made which greatly reduce the computational effort required for simulating thermoluminescence response curves measured under various different experimental conditions. The justification for these assumptions is discussed in detail in Sec. IV. Here we only briefly review the important features of the simplified theory.

Assume a system that consists of a thermoluminescent phosphor layer on a glass substrate in perfect thermal contact. Each layer is characterized by its optical absorption coefficient μ_i , thermal conductivity k_i , and thickness l_i . The index $i = 1, 2$ denotes the respective layer and the total thick-

ness is $L = l_1 + l_2$. In contrast to the general theory, we assume for the special case of a thin phosphor layer on a thicker glass slide that the thermal diffusivity α , is temperature independent and identical for both layers. The laser beam has a fixed diameter and a uniform circular intensity profile which is cylindrically symmetric around the beam axis. It enters the two-layer system perpendicular to the x - y plane either from the side of the phosphor layer or the glass substrate. The absorbance (absorbed fraction of the inci-

dent laser power) is of course different in both cases, and so is the prefactor B in the expression for the temperature rise [Eq. (1) below]. The thermal diffusion equation and the appropriate boundary and initial conditions for this problem are stated in Ref. 8.

Accounting for first-order reflection losses on the surface of incidence and at the layer interface, the spatial and temporal distribution of the temperature rise for the two layers is given by⁸

$$\begin{aligned} \Delta T_i(r,z,t) = & (BP^*/\omega^2) \int_0^t d\tau Q(r,t-\tau) \left(1 + [(1-R_i)/\pi B] \right. \\ & \times \sum_{m=1}^{\infty} \exp(-\mu_m l_1) [\exp(\mu_m l_1) - \cos(\eta_m l_1) + (\eta_m/\mu_m) \sin(\eta_m l_1)] \\ & \times [N_m (1 + \eta_m^2/\mu_m^2) \cos(\eta_m l_1)]^{-1} + (1-R_2) \exp(-\mu_m l_1) \\ & \times [\cos(\eta_m l_2) + (\eta_m/\mu_m) \sin(\eta_m l_2) - \exp(-\mu_m l_2)] \\ & \left. \times [N_m (1 + \eta_m^2/\mu_m^2) \cos(\eta_m l_2)]^{-1} \right) x_i(z) \exp[-\alpha \eta_m^2 (t-\tau)]. \end{aligned} \quad (1)$$

where P^* is the total laser power (not the power density) incident on the front surface, R_i the reflectivity of layer i , and ω the radius of the uniform circular beam. We further have

$$B = (1-R_1) [1 - (1-R_2) \exp(-\mu_1 l_1 - \mu_2 l_2) - R_2 \exp(-\mu_1 l_1)] / \pi N_0,$$

$$N_0 = (1/\alpha) \sum_{i=1}^2 k_i l_i,$$

and

$$N_m = \frac{1}{2} \sum_{i=1}^2 k_i l_i [1 + \sin(2\theta_i)/2\theta_i] \cos^2(\theta_i)$$

with $\theta_i = \eta_m l_i$, and $Q(r,t) = P(\omega/\sqrt{2\alpha t}, r/\sqrt{2\alpha t})$.

$$P(\omega,r) = \int_0^\omega \omega' d\omega' I_0(\omega',r) \exp[-(\omega'^2 + r^2)/2]$$

is called the circular coverage function, and

$$x_1(z) = \cos(\eta_m z) / \cos(\eta_m l_1)$$

and

$$x_2(z) = \cos[\eta_m (L-z)] / \cos(\eta_m l_2).$$

The parameters η_m ($m = 1, 2, \dots$) are the roots of the following transcendental equation (see the Appendix):

$$k_1 \tan(\eta_m l_1) + k_2 \tan(\eta_m l_2) = 0, \quad (2)$$

which arises from the boundary conditions.

An additional simplification of Eq. (1) is possible. It stems from the fact that the material of interest in our studies, LiF, is not a strong absorber for the 10.6- μm photons of the laser heating beam ($\mu = 40 \text{ cm}^{-1}$). In contrast to this, the absorption coefficient of the glass substrate is high ($\sim 10^4 \text{ cm}^{-1}$). Consequently, the laser deposits the energy directly into the interface between the layers if it impinges on the phosphor side of the two-layer system (case 1 below). On the other hand, it is possible to direct the laser beam onto the glass side of the system where it is completely absorbed at the surface (case 2). Thus the active thermoluminescent layer can be located between $z = 0$ and $z = l_1$ (case 1) or between $z = l_1$ and $z = L$. The appropriate expressions for the temperature rise in these cases are readily obtained from Eq. (1).

Case 1. Thermoluminescent layer on top of the glass substrate ($\mu_1 l_1 \ll 1$):

$$\Delta T_1(r,z,t) = (BP^*/\omega^2) \int_0^t d\tau Q(r,t-\tau) \left(1 + N_0 \sum_{m=1}^{\infty} \cos(\eta_m z) \exp[-\alpha \eta_m^2 (t-\tau)] / [N_m (1 + \eta_m^2/\mu_m^2) \cos(\eta_m l_1)] \right). \quad (3)$$

Case 2. Thermoluminescent layer at the bottom of the glass substrate ($\mu_2 l_2 \ll 1$):

$$\begin{aligned} \Delta T_2(r,z,t) = & (BP^*/\omega^2) \int_0^t d\tau Q(r,t-\tau) \left(1 + N_0 \sum_{m=1}^{\infty} \cos[\eta_m (L-z)] \right. \\ & \left. \times \exp[-\alpha \eta_m^2 (t-\tau)] / [N_m (1 + \eta_m^2/\mu_m^2) \cos(\eta_m l_1) \cos(\eta_m l_2)] \right). \end{aligned} \quad (4)$$

The actual computer calculations of the thermoluminescence response are based on the well-known first-order electron kinetics of the LiF:Mg,Ti phosphor (TLD-100, Harshaw/Filtrol) and require knowledge of the heating rates in each volume element $2\pi r dr dz$ given as follows:

Case 1 ($\mu_1 l_1 \ll 1$):

$$\partial T_1(r,z,t)/\partial t = (BP^*/\omega^2)Q(r,t) \left(1 + N_0 \sum_{m=1}^{\infty} \cos(\eta_m z) \exp(-\alpha \eta_m^2 t) / [N_m (1 + \eta_m^2 \mu_2^2) \cos(\eta_m l_1)] \right). \quad (5)$$

Case 2 ($\mu_2 l_2 \ll 1$):

$$\partial T_2(r,z,t)/\partial t = (BP^*/\omega^2)Q(r,t) \left(1 + N_0 \sum_{m=1}^{\infty} \cos[\eta_m (L - z)] \exp(-\alpha \eta_m^2 t) / [N_m (1 + \eta_m^2 / \mu_1^2) \cos(\eta_m l_1) \cos(\eta_m l_2)] \right). \quad (6)$$

The luminescence glow peaks of the LiF:Mg,Ti considered are commonly called peaks 3, 4, and 5. They are well described by first-order kinetics with attempt-to-escape frequencies of 4×10^{13} , 7.3×10^{15} , and $4 \times 10^{21} \text{ s}^{-1}$ and trap depths of 1.23, 1.54, and 2.17 eV, respectively.⁹

The sum of the relative peak heights⁹ of the LiF:Mg,Ti glow curve is used as a measure for the total trapped electron population, and the relative population of each of the three electron trap levels is taken to be proportional to its corresponding peak height with the correction of luminescence efficiency at different heating rates.¹⁰ TL peaks that occur at temperatures lower than those of peaks 3-5 are eliminated by a preannealing for 10 min at 100 °C.

The three first-order electron-kinetic differential equations for peaks 3-5 (Ref. 9) are solved with these heating rates by the Runge-Kutta method for each volume element $2\pi r dr l_1$ (for case 1) or $2\pi r dr l_2$ (for case 2). Because the phosphor layer is very thin, integration over the phosphor layer thickness is omitted (see Fig. 10 below). In Sec. IV this

assumption will be justified by comparison of measured and calculated thermoluminescence response curves. The numerical integration is sufficiently precise with step sizes $\Delta r = 1.25\omega/50$ and $\Delta t = 10^{-3} \text{ s}$ except for the first millisecond during which $\Delta t = 10^{-6} \text{ s}$.

III. EXPERIMENTAL PROCEDURE

The experimental arrangement is schematically shown in Fig. 1. A temperature-stabilized radio-frequency-excited cw CO₂ laser (Directed Energy Inc. Model L35-PS) emits a beam whose intensity profile has an annular ("halo") cross section of 1 cm diameter. The 10.6- μm laser beam is linearly polarized. The maximum output power is 40 W. For closed-loop control of the laser beam, the rf power supply is modified for pulse-width modulation at 34 kHz with a variable duty cycle that determines the laser output power.

The beam is guided to a focusing module by two parallel gold-coated copper mirrors. It enters the light-tight optical

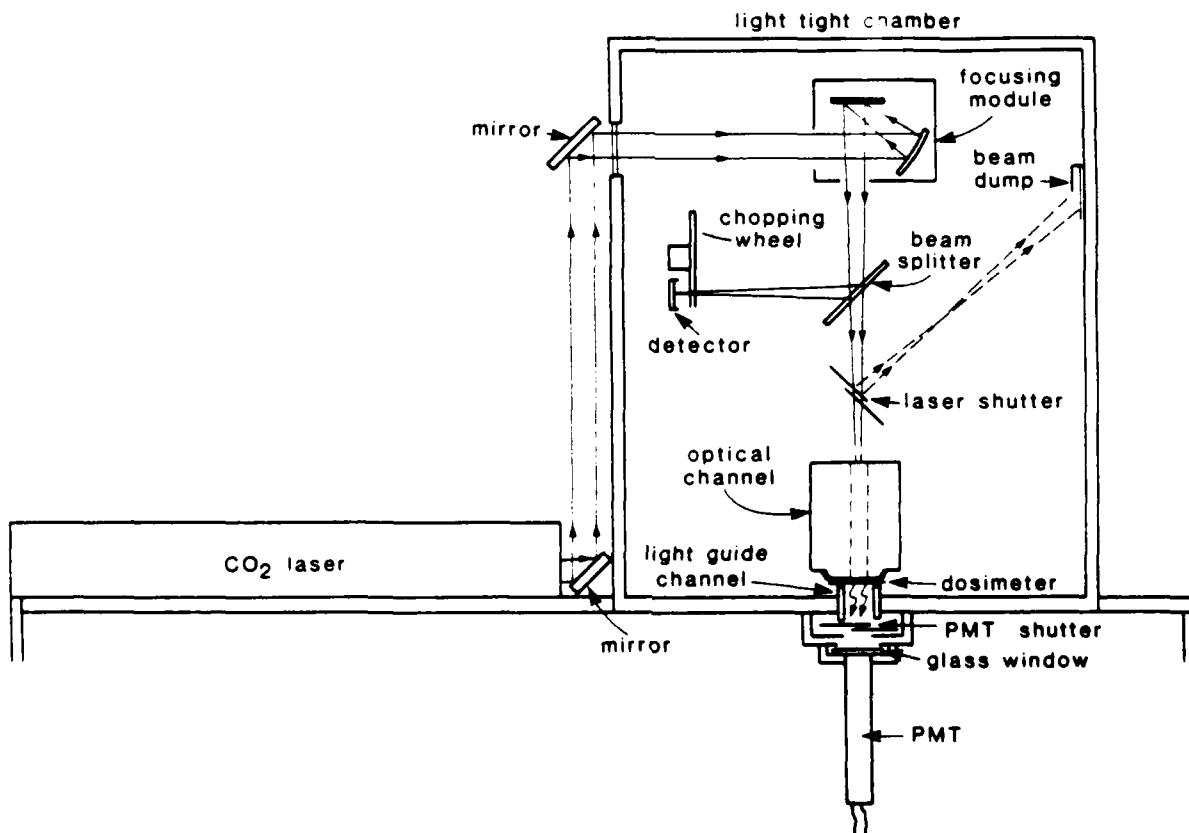


FIG. 1. Schematic experimental arrangement of the laser thermoluminescence apparatus.

chamber through an antireflection-coated Ge window. The focusing module deflects the beam down onto the entrance of the beam equalizer channel,⁶ which produces a uniform square beam of $3 \times 3 \text{ mm}^2$ area. To simplify the theory and the numerical calculation, the square profile of the output beam is converted to a circular one with the aid of a 2.95-mm-diam aperture at the channel exit. The sample holder is placed in close proximity to it so that, at the top of the sample, the beam has diverged only to about 3 mm diam.

A gold-plated electromechanical shutter, placed in front of the channel, controls the exposure time of the sample to the laser beam. When it is closed, the laser beam is reflected into a beam dump.

To provide a signal for closed-loop control of the laser power, an antireflection coated ZnSe window reflects a small fixed portion (3–5 %) of the laser beam to a piezoelectric detector (Barnes Engineering Inc. Model 350-5 PZT). A beam-chopping wheel operated at 33.5 Hz by a dc motor is placed in front of the detector in order to prevent saturation. The output of the detector is fed to the electronic control unit, providing an updated laser power measurement every 9.3 ms. In this way, the laser output power is kept constant within 2–3 %.

A TL sample on a $25 \times 25\text{-mm}^2$ substrate can be placed in a sample holder at a distance of 40–50 μm from the end of the channel. A specific area of the sample, selected by a pair of coupled translation stages, can be heated by the laser beam. Typical exposure times range from 100 ms to 10 s. The

translation stages are connected to two motor driven actuators which are controlled by a motor drive system with a positioning accuracy of up to 0.1 μm .

As in Ref. 1, we have chosen LiF:Mg,Ti (TLD-100 supplied by Harshaw/Filtrol) as the thermoluminescent material to serve as a monitor of the temperature evolution when the two-layer system is exposed to the laser beam. All the systems which are studied to-date have consisted of a 35–40- μm -thick fine-grain phosphor layer in a high-temperature binder on 150- μm -thick borosilicate glass microscope cover slides. After exposure to ^{60}Co γ rays (for the purpose of filling the traps) and a subsequent 10-min preanneal treatment to eliminate low-temperature glow peaks,¹ the center of these samples was heated with a stable and uniform $3 \pm 0.07\text{-mm}$ -diam CO_2 laser beam with power output between 2.44 W and 13.5 W. The laser exposure was done in two different modes, the laser beam either striking the front (phosphor layer) or the back (substrate). Naturally, the prefactor B (see Sec. II), is different for these two modes of laser exposure. With the method described in Ref. 1 its value was determined to be $B = 10.7 \pm 25\% \text{ K cm}^2/\text{J}$ for the phosphor layer surface and $B = 6.3 \pm 20\% \text{ K cm}^2/\text{J}$ for the glass substrate surface (note that B is defined slightly differently since here it is divided by the laser power P^*).

The emitted light from a TL sample is transmitted by a light guide,³ through a shutter, and a protective glass window to a photomultiplier tube (PMT, EMI type 9924B). The shutter and glass plate prevent the PMT from accidental

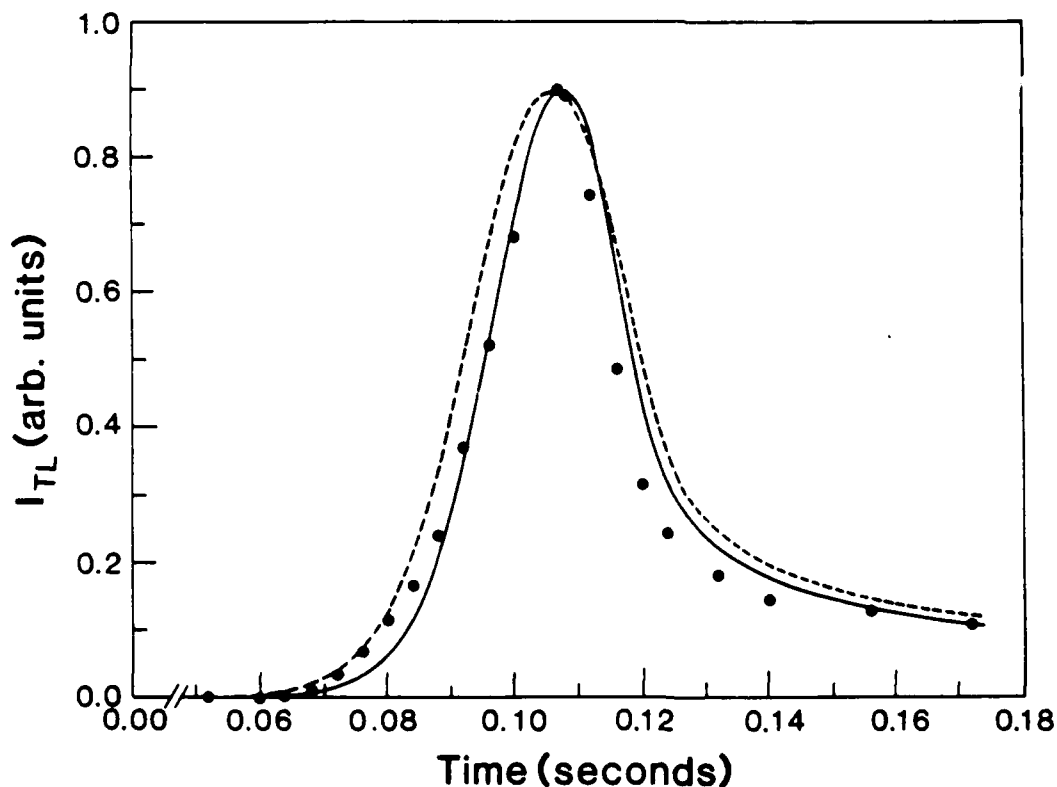


FIG. 2. Thermoluminescence response curves measured and calculated with a uniform laser beam of 3 mm diameter and 9.75 W power heating at 37.5- μm -thick TL layer through a 0.15-mm-thick borosilicate glass substrate (the laser beam impinges onto the glass substrate). The solid line is computed with a constant thermal conductivity of the glass $k = 0.00942 \text{ W/K cm}$ and the dashed line with the method of the Kirchhoff transformation, which takes into account the temperature dependence of k (Ref. 1). With the thermal diffusivity $\alpha = 0.0064 \text{ cm}^2/\text{s}$ (see Fig. 3), the parameter B was determined to be $6.4 \text{ K cm}^2/\text{J}$ by fitting to the peak of the measured curve. This value agrees well with the experimentally determined one: $B = 5.7 \pm 20\% \text{ K cm}^2/\text{J}$ (see Ref. 1). Prior to the measurement of the TL response curve, the sample was exposed to γ rays from a ^{60}Co source and preannealed for 10 min at 100°C .

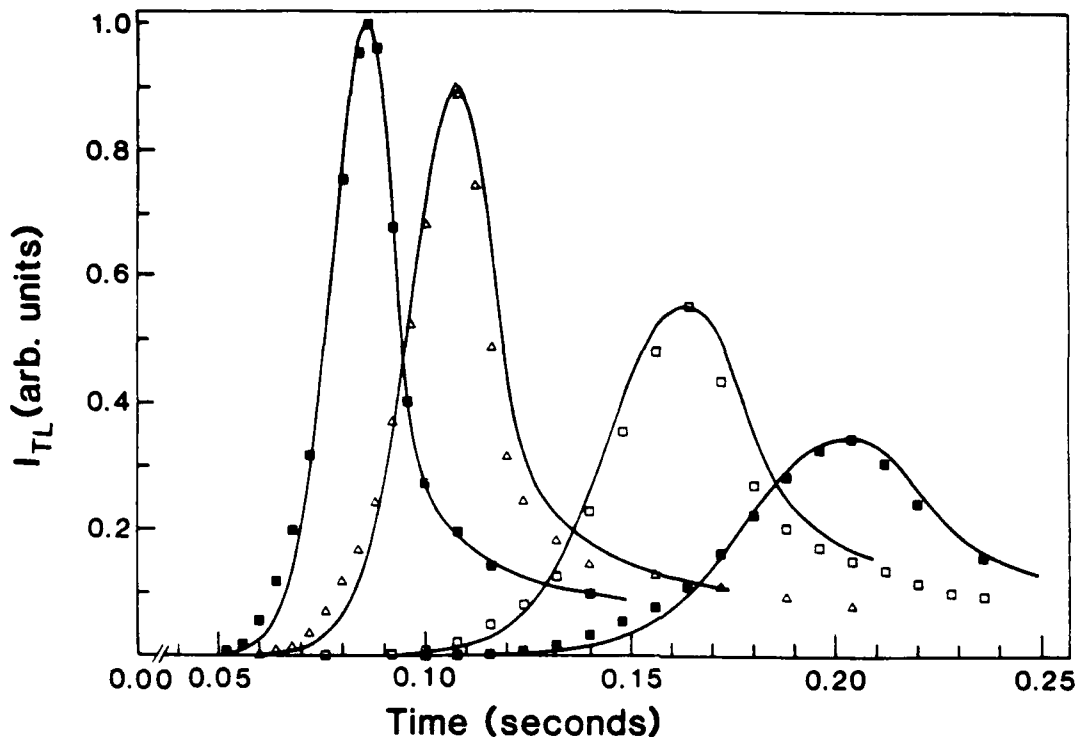


FIG. 3. Thermoluminescence response curves measured by heating with laser beams of fixed 3 mm diam but different powers impinging onto the glass side of the two-layer system. The sample is a 37.5- μm -thick LiF:Mg,Ti on a 0.15-mm-thick borosilicate glass substrate. The family of curves, calculated from Eqs. (4) and (6), yields the value $\alpha = 0.0064 \text{ cm}^2/\text{s}$ for the thermal diffusivity via the best fit matching the shape after peak position. The calculations were performed with $k_1 = 0.00942 \text{ W/K cm}$ that is characteristic for the system and the following B parameters and laser power: $B = 6.3, 6.4, 6.0,$ and $6.3 \text{ K cm}^2/\text{J}$ at $P^* = 13, 9.75, 6.5,$ and 4.875 W , respectively. Peaks 1 and 2 of LiF:Mg,Ti (TLD-100, Harshaw/Filtrol) were removed by 10 min preannealing at 100°C (Ref. 9).

exposures to visible light or the unimpeded laser power, respectively. To maximize the collection efficiency of the emitted thermoluminescence, one end of it is placed in close proximity to the heated area on the sample. The current signal of the PMT is measured, processed, stored, and displayed with the aid of a transient digitizer.

The electronic control unit of the apparatus performs such functions as timing, controlling, and protecting the system. When a TLD reader heating cycle is activated, the following sequence is performed:

The laser is turned on and its output power is measured and adjusted until the laser is stabilized at the desired power

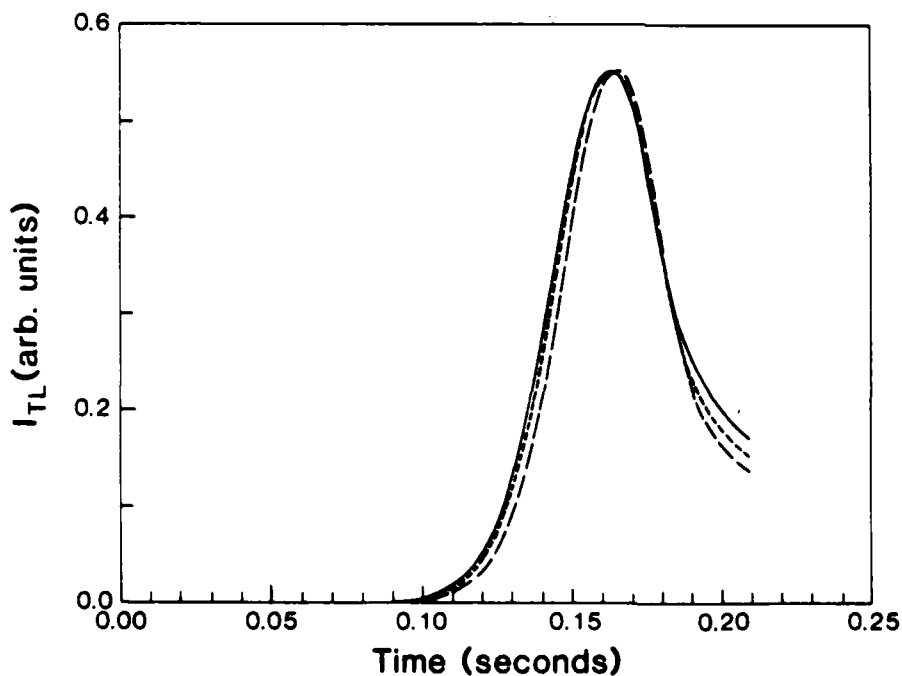


FIG. 4. Computed thermoluminescence response curves of the sample from Fig. 3 for various thermal diffusivities α . This fit with the measured curve is obtained with $\alpha = 0.0064 \text{ cm}^2/\text{s}$ and the prefactor $B = 6.0 \text{ K cm}^2/\text{J}$ (dotted curve). The effect of different thermal diffusivities is demonstrated by the solid ($\alpha = 0.005 \text{ cm}^2/\text{s}$) and the dashed ($\alpha = 0.0078 \text{ cm}^2/\text{s}$) lines. Laser power $P^* = 6.5 \text{ W}$.

level. This process is normally accomplished in 100–300 ms; however, it may require a longer time if the laser happens to be in an undesirable operating condition. During this time, the shutter remains closed and the sample is not exposed to the beam. After the desired laser power is obtained, the shutter is open for a set desired heating time. At the end of the heating cycle, the shutter closes and the laser is turned off.

IV. RESULTS AND DISCUSSION

In an initial set of tests we established the validity of a number of assumptions and approximations made to reduce the computational effort required for the comparison of experiments and the theory. The first of these approximations concerns the method of the Kirchhoff transformation described in Ref. 1. It permits one to account for the temperature dependence of the thermal conductivity of the glass substrate, which we approximated as $k_2 = 0.00942(1 + 0.00222\Delta T_2)$ W/K cm, based on data given by the glass manufacturer.¹¹ Figure 2 shows the TL response curve that was measured by exposing the glass layer (case 2: heating from the back of the sample) to a 9.75-W laser beam together with calculations based on Eqs. (4) and (6) and in conjunction with the simplifying assumptions discussed below. The Kirchhoff transformation yielded the dashed line, and the solid line was obtained assuming constant $k_2 = 0.00942$ W/K cm and with constant diffusivity $\alpha = 0.0064$ cm² s⁻¹. In view of the rather good agreement between theory and experiment that is achieved without accounting for the temperature dependence of k , we decided to disregard the Kirchhoff transformation for all cases described in this paper. We have checked this with a number of different experimental situations and found it was always justified in applications of the theory of Ref. 8 to thin two-layer thermoluminescence dosimeter configurations.

The phosphor layer is indirectly heated by diffusion, which is rather rapid in the z direction, because its thermal response time or diffusion time,¹² $t_0 = l^2/\alpha$, is estimated to be about 1 ms. This is much shorter than the time required to measurably change the thermoluminescence intensity even at the highest laser power densities that appear practical for this type of heating in thermoluminescence dosimetry.⁷ Assuming the thermal diffusivity of the phosphor layer is not significantly greater than that of the glass substrate, heat transport by lateral thermal diffusion occurs mainly in the thicker of the two layers with essentially instantaneous diffusion in the z direction through the thin layer. This is of course also true for case 2 (laser heating from the back). Therefore, we are justified in assuming the thermal diffusivity of both layers to be equal, its value being that of glass.³ Actually, there is a reason to assume that the thermal diffusivity of the phosphor layer is rather small, perhaps even smaller than that of glass. This layer is a loosely packed matrix of small grains in a poor heat conductor (Dow Corning 805 silicone).

The thermal diffusivity α for glass is slightly temperature dependent (varying from 0.0052 cm²/s at 0°C to 0.0057 cm²/s at 100°C, but it is unknown for higher temperatures), and since we did not choose to account for this, we had the problem of selecting a proper "temperature-aver-

aged" value that provided a good approximation for all calculations presented below. We established that value as $\alpha = 0.0064$ cm²/s by fitting of families of TL response curves measured for front and back exposure with several different laser powers (Fig. 3 is an example). This high value appears justified when one considers the fact that the TL glow peaks we selected as "temperature indicators" for our experiments reach their maximum emission intensity at about 250°C.⁹ Consequently, the major portion of the thermoluminescence emission and thus the range of "temperature monitoring" occurs well above 100°C. The high-temperature side of the glow curve is very sensitive to the value of α as shown in Fig. 4 and our choice is the best match to this shape.

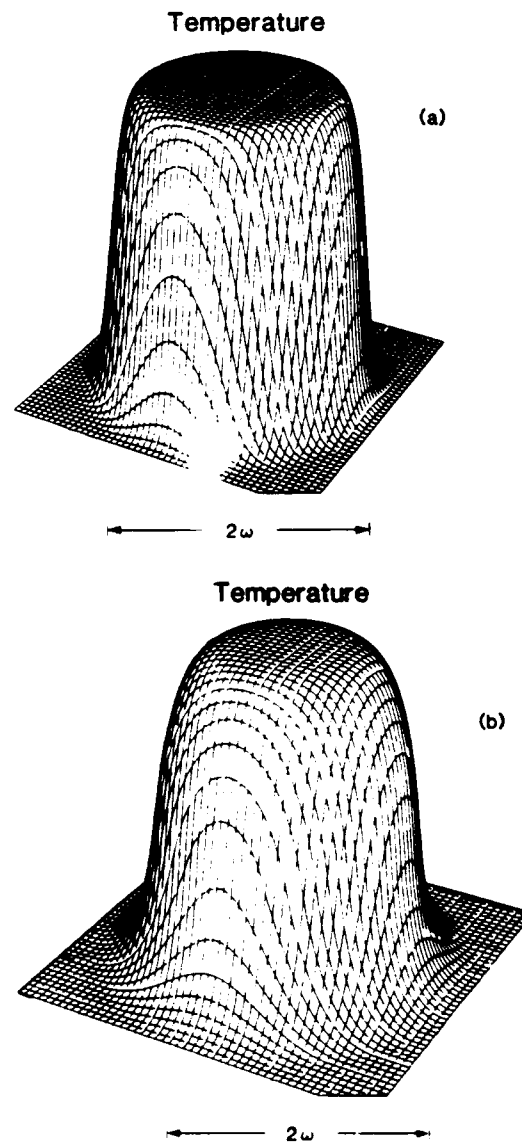


FIG. 5. Computer simulations for the normalized spatial temperature distributions $T(r,z,t)$ calculated for exposure of a phosphor layer on a glass substrate to a 6.5-W laser heating beam with a uniform circular intensity profile, $2\omega = 3$ mm. The calculations are performed with $B = 7.55$ K cm²/J, $\alpha = 0.0064$ cm²/s, and a total thickness $L = 0.1875$ mm for various times after onset of laser exposure: (a) $t = 4$ ms and (b) $t = t^* = 115$ ms (the peak intensity of the thermoluminescence response occurs at t^*).

Yet another simplification of the computational procedure is possible because the TL phosphor layer is so thin and diffusion across it is relatively rapid. Instead of calculating the transient TL emission from infinitesimally thin layers δz and integrating over z from $z = 0$ to $z = l_1$, it suffices to calculate the TL emission either from the surface layer at $z = 0$ or from the interface layer at $z = l_1$. The total instantaneous emission is then obtained simply by multiplying with the thickness, l_1 , of the active layer. In each situation good agreement between theory and measurements is obtained.³ Henceforth, we arbitrarily choose to take the computed TL emission from the interface at $z = l_1$ to represent the emission from the entire layer.

We repeat, these simplifications were introduced solely to reduce the computational effort. The calculations have yielded results that agree with measurements within the ex-

perimental errors. The more exact calculations pose no problems in principle.

Even though we have not yet measured in detail spatially resolved thermoluminescent responses from a TL phosphor layer on a glass slide that is heated with a localized uniform laser beam, we present here some initial computational results as they help to visualize the relation between the spatial and temporal temperature distribution and the corresponding thermoluminescent response. Figure 5(a) shows the temperature distribution in the phosphor-glass interface at $t = 4$ ms after onset of exposure of the phosphor layer to a uniform 3-mm-diam laser beam of 6.5 W power. Figure 5(b) shows the temperature distribution at $t = t^* = 115$ ms (here t^* is the time of TL peak occurrence). The distribution is considerably different due to heat diffusion. Interestingly, the lateral distribution of the TL emis-

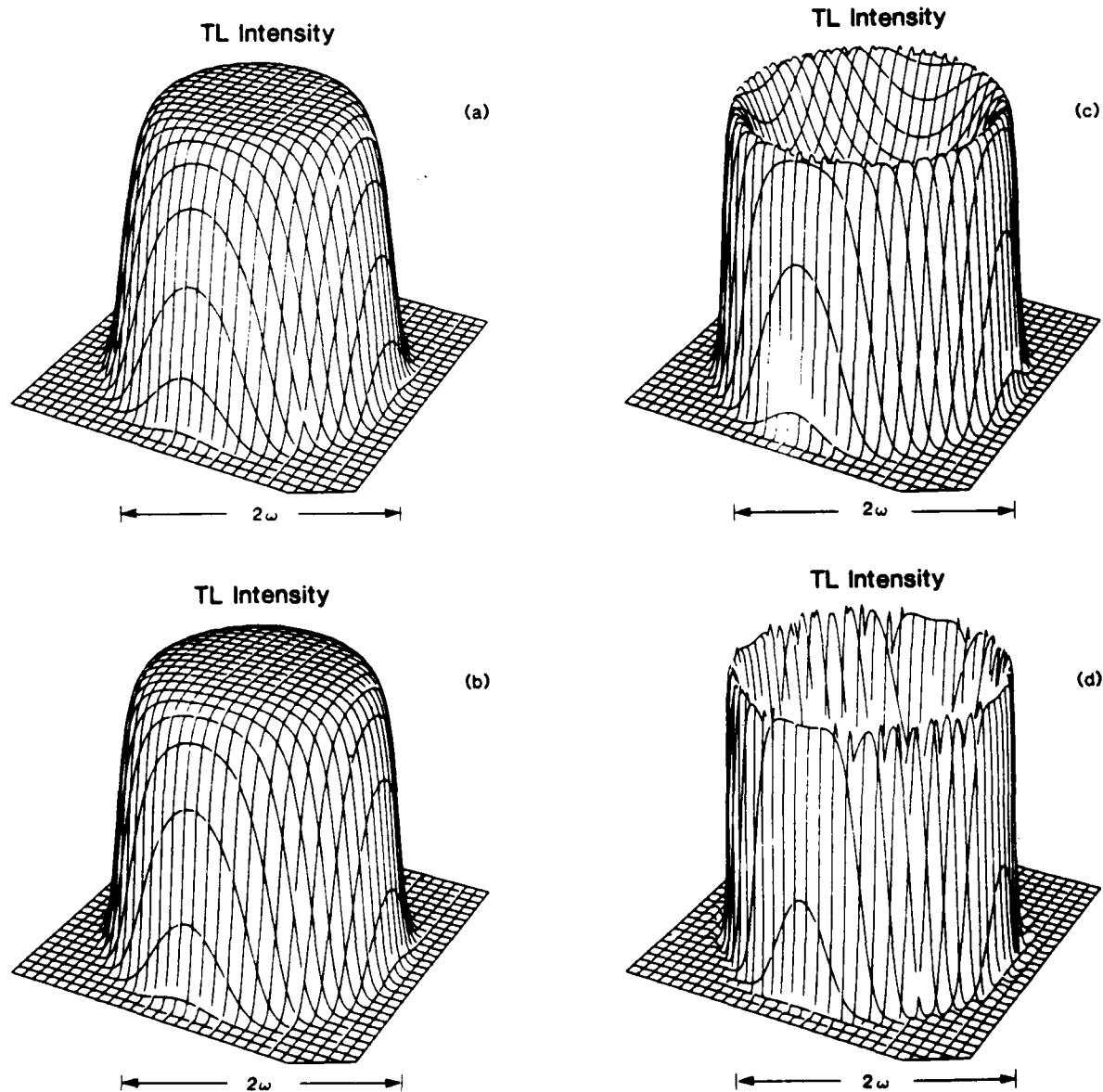


FIG. 6. The normalized spatial distributions of the thermoluminescence response calculated for the sample from Fig. 6 at various times t with respect to the time, t^* , of the TL peak intensity occurrence: (a) $t = \frac{1}{2}t^*$, (b) $t = t^*$, (c) $t = 1.1t^*$, and (d) $t = 1.5t^*$.

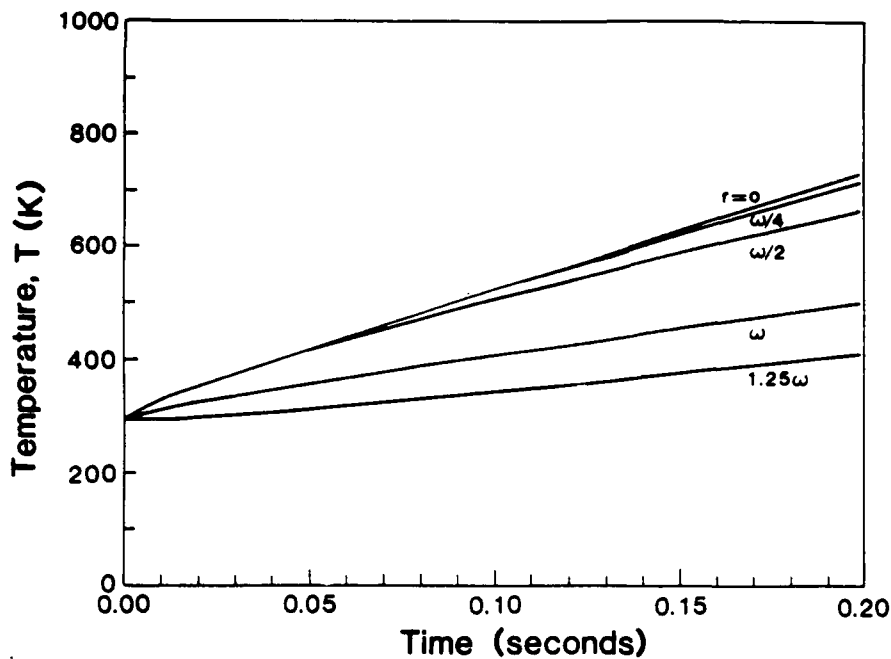


FIG. 7. Computed time evolution of the temperature of the sample and experimental conditions in Fig. 6 at various distances r from the laser beam axis: $r = 0, \omega/4, \omega/2, \omega,$ and 1.125ω (from top to bottom). ($\omega = 0.15$ cm is the radius of the laser beam.)

sion retains the basically cylindrical shape up to t^* ; it simply broadens with heating time. This is of course a result of the initial rise of a glow curve which is proportional to $\exp(-E/kT)$ (E is the thermal activation energy). Immediately after t^* , the TL intensity decreases in the central and hottest part of the exposed area and becomes essentially zero at $t = 1.5t^*$, shown in Figs. 6(a)–6(c). For times $t > 1.25t^*$, the TL emission originates only from those areas of the phosphor layer that are not directly exposed to the laser beam, but are heated by lateral diffusion.

For applications of laser heating in thermoluminescence dosimetry it is of interest to investigate the temperature rise

of the exposed phosphor layer. Optimum operating conditions are commonly believed to include heating a thermoluminescent dosimeter with a constant heating rate; i.e., a temperature rise linear in time.¹³ Figure 7 shows computed temperature rise curves for the same sample and experimental conditions discussed above. In agreement with calculations by Sparks,¹² the temperature in the center of the exposed spot rises first nonlinearly for a few ms and is linear thereafter. The heating rate is proportional to the laser power. The numerical calculations indicate further, that the heating rate is very nearly the same for an area centered around the laser beam axis up to a radius 0.5ω for heating

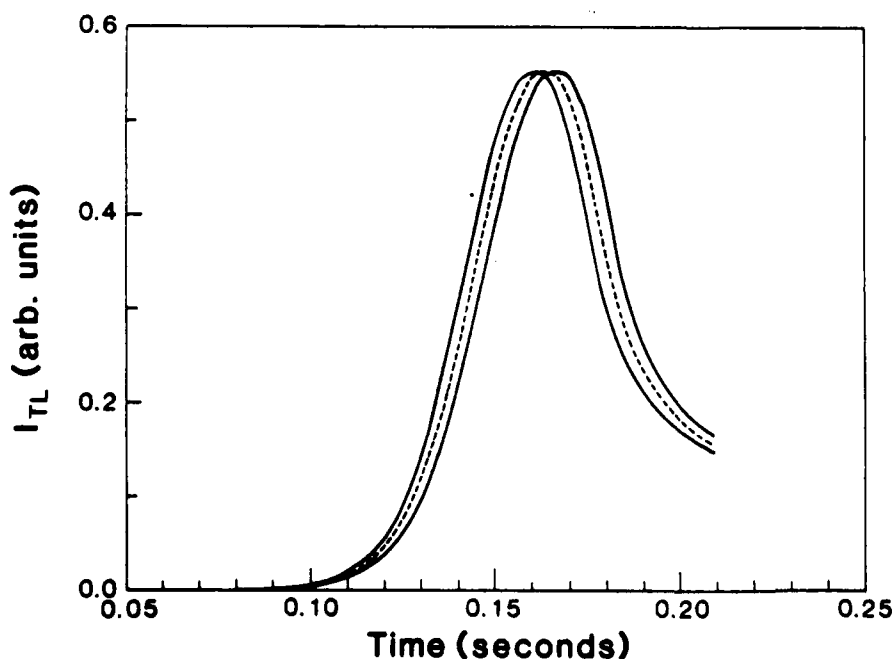


FIG. 8. Calculated thermoluminescence response curves of the sample from Fig. 3 for a small variation in the radius of the laser beam. The computations are performed with $P^* = 6.5$ W and the following beam radii ω (from left to right): 0.1485, 0.15, and 0.1515 cm.

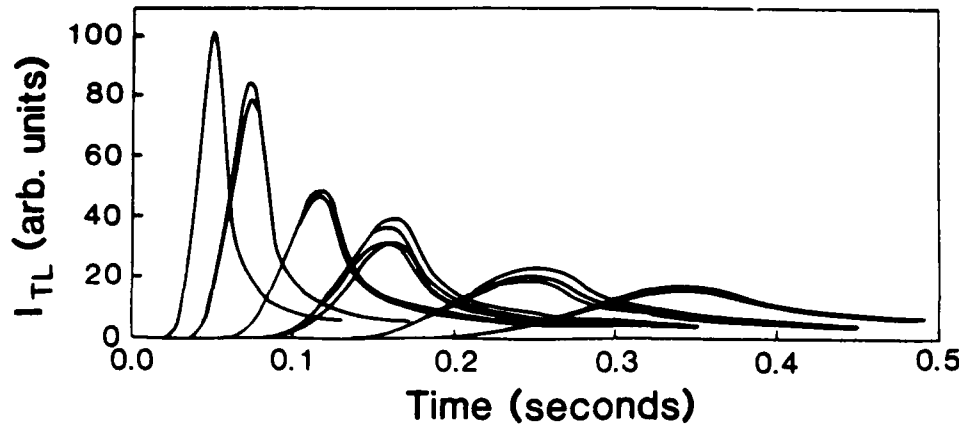


FIG. 9. A set of thermoluminescence response curves measured with a 37.5- μ m-thick TL layer on 0.15-mm-thick borosilicate glass substrate for fixed laser beam radius $\omega = 0.15$ cm and various laser powers P^* . The laser beam impinges on the phosphor side of the sample. To check the reproducibility of the measurements, several thermoluminescence responses from different sites on the sample were measured for otherwise identical conditions with the following laser powers (in W): 13.9, 7.5, 6.5, 4.875, 3.25, and 2.44 (from left to right).

times well past the peak of the TL glow curve (compare with Figs. 4–6). This is of considerable practical importance as it demonstrates the usefulness of laser heating not only for dosimetry,^{3,14} but also in a number of special areas which exploit thermoluminescence, e.g., dating of archaeological artifacts and art authentication.¹⁵ Very precise linear and reproducible heating is possible of minute fine-grain samples that are attached with a suitable binder to a substrate in the center of the uniform laser heating beam. The reproducibility and accuracy of this heating technique depend, of course,

on the stability and reproducibility of the laser beam. As mentioned in Sec. III, it is possible to control the laser power to within 3%.

Experimental errors arise from the uncertainty in laser beam parameters, the phosphor layer uniformity, and the reproducibility with which the two-layer samples can be produced. With a stable laser power, only the beam radius ω remained as a critical parameter. Calculations indicated that it very sensitively influences the TL glow curves. Figure 8 shows that changing ω by only $\pm 1\%$ yields shifts in peak

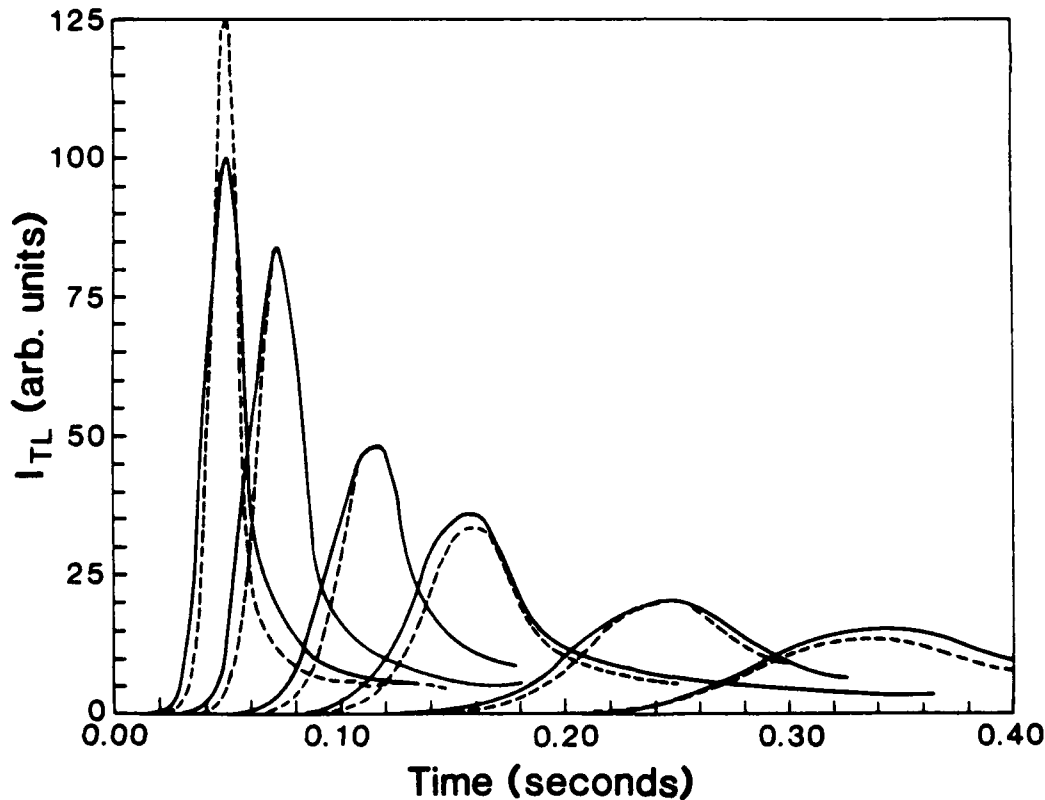


FIG. 10. Measured and computed thermoluminescence response curves of the sample from Fig. 9, and the same experimental conditions. The dashed curves are computed from Eqs. (3) and (5) and the first-order electron kinetics parameters determined by McKeever (Ref. 9) for peaks 3–5 of LiF:Mg,Ti and by taking into account the measured decrease in luminous efficiencies with increasing heating rates. Again, peak 2 was removed by a 10-min preannealing at 100 °C. With the thermal diffusivity $\alpha = 0.0064$ cm²/s and a laser beam radius of $\omega = 0.15$ cm, the parameter B was determined for each curve by the best fit. The results are calculated with the following luminescence efficiencies η (in % of the value obtained for the smallest heating rate): 81.8, 81.9, 85.5, 89.6, 95.7, and 100 (from left to right). The parameters B (k cm²/J) are: 8.53, 7.93, 7.55, 7.30, 7.17, and 7.00 (from left to right).

occurrences that otherwise are produced only by variation of the produced layer thicknesses.

Variations in the thickness, l_1 , of the phosphor layer cause the TL response curves to shift and change in intensity. This is demonstrated in Fig. 9, which shows a number of curves that were measured with different values of l_1 . Figure 9 indicates the rather limited reproducibility of the spreading method used to fabricate the samples. Despite considerable effort, which involved the construction of a special layer spreading machine and careful control of the phosphor-binder mixture, this performance could not be improved beyond the one reported here, and more work on layer fabrication techniques is needed. However, the layer uniformity achieved was sufficient for a study of the TL response of a number of nominally identical samples as a function of laser power. Typical measured and computed glow curves resulting from this study as shown in Fig. 10 (case 1: the laser heating beam impinges onto the TL layer). The parameter B had to be adjusted slightly, but note that the variation in B is within the accuracy of the experimental method we used to determine it.¹ It was also necessary to account for the fact that the overall luminescent yield decreases with increasing heating rate for otherwise identical experimental conditions. Details of the dependence of the yield on the heating rate will be presented in a forthcoming publication.^{3,10}

V. CONCLUDING REMARKS

We have compared experimental and computed thermoluminescence response curves obtained from two-layer configurations by localized heating with a 3-mm-diam CO₂ laser beam of uniform circular intensity profile of power up to 13 W. The results confirm the theory of Ref. 8 and show that thin-layer thermoluminescence dosimeters can be heated with heating rates up to 5500 °C/s.

It is of particular importance that the thermoluminescence glow curves measured under these experimental conditions have the familiar shape obtained with conventional contact heating.

ACKNOWLEDGMENTS

This work was supported by the Office of Naval Research under Contract No. N00014-82-K-0529. The authors wish to thank members of the Division of Physics, NRC. In particular, Dr. J. Young and Dr. R. Normandin for many helpful suggestions and Dr. C. Jacques and Dr. G. Aers for use of their three-dimensional plotting software.

APPENDIX

In this work we have a poorly absorbing phosphor coating $l_1 = 0.2L$ on a highly absorbing glass slide, $l_2 = 0.8L$

where the total thickness $L = 0.01875$ cm. In this case m distinct roots η_m can be obtained from the transcendental equation $k_1 \tan \theta + k_2 \tan 4\theta = 0$ with $\theta = 0.2\eta_m L$. With $F = 5\pi/L$, $h = 3 + 2/k$, $k = k_1/k_2$,

$$D^+ = \{h + [h^2 - (1 + 4/k)]^{1/2}\}^{1/2},$$

and

$$D^- = \{h - [h + (1 + 4/k)]^{1/2}\}^{1/2},$$

then the m roots greater than $\eta_0 = 0$ are given by

$$\eta_m = \begin{cases} [\pi^{-1} \tan^{-1}(D^-) + (m-1)/5]F & \text{for } m = 1, 6, 11, \dots \\ [\pi^{-1} \tan^{-1}(D^+) + (m-2)/5]F & \text{for } m = 2, 7, 12, \dots \\ [1 - \pi^{-1} \tan^{-1}(D^+) + (m-3)/5]F & \text{for } m = 3, 8, 13, \dots \\ [1 - \pi^{-1} \tan^{-1}(D^-) + (m-4)/5]F & \text{for } m = 4, 9, 14, \dots \\ mF/5 & \text{for } m = 5, 10, 15, \dots \end{cases}$$

The root $\eta_0 = 0$ yields the first term, unity, in the large parentheses of Eq. (1).

- ¹A. Abtahi, P. Braunlich, and P. Kelly, *J. Appl. Phys.* **58**, 1626 (1985).
- ²P. Braunlich, editor, *Thermally Stimulated Relaxation in Solids* (Springer, Heidelberg, 1979).
- ³A. Abtahi, Ph.D. dissertation, Washington State University, 1986.
- ⁴Y. Yasuno, H. Tsutsui, O. Yamamoto, and T. Yamashita, *Jpn. J. Appl. Phys.* **21**, 967 (1982).
- ⁵P. Braunlich, W. Tetzlaff, J. Gasiot, and S. Jones, in *Proceedings of the International Beta Dosimetry Symposium*, Washington, DC, 1983, U. S. Nuclear Regulatory Commission Publication No. NUREG/CP-00500, p. 293.
- ⁶P. Braunlich and W. Tetzlaff, Patent Pending, Serial No. 652,829, Case No. US-5 (1985).
- ⁷P. Braunlich and W. Tetzlaff, presented at the 8th International Conference on Solid State Dosimetry, Oxford, U.K., August, 1986.
- ⁸A. Abtahi, P. Braunlich, and P. Kelly, *J. Appl. Phys.* **60**, 3417 (1986).
- ⁹S. W. S. McKeever, *Nucl. Instrum. Methods* **175**, 19 (1980).
- ¹⁰A. Abtahi, P. Braunlich, T. Haugan, and P. Kelly, presented at the 8th International Conference on Solid State Dosimetry, Oxford, U.K., August, 1986.
- ¹¹Erie Scientific, Division of Syborn Corp., Portsmouth Industrial Park, Portsmouth, NH 03801.
- ¹²M. Sparks, *J. Appl. Phys.* **47**, 837 (1976).
- ¹³M. Oberhofer and A. Scharmann, editors, *Applied Thermoluminescence Dosimetry* (Hilger, Bristol, 1981).
- ¹⁴W. Tetzlaff, P. Braunlich, and K. Swinth, *Proceedings of the DOE Workshop on Beta Measurement*, Albuquerque, 1986 (to be published).
- ¹⁵M. J. Aitkin, *Physics and Archaeology*, 2nd ed. (Clarendon, Oxford, 1974).

Transient solution of the diffusion equation for a composite system heated with a laser beam

J. F. Young and P. Kelly

National Research Council of Canada, Division of Physics, Ottawa, Ontario K1A 0R6, Canada

A. Abtahi,^{a)} P. F. Braunlich, and S. C. Jones

Department of Physics, Washington State University, Pullman, Washington 99164-281

(Received 6 April 1989; accepted for publication 9 August 1989)

The general solution of the thermal diffusion equation for the case of a semi-infinite two-layer system that is heated with a localized cw laser beam of circularly uniform intensity profile is extended to times after the pulse is switched off. An application of that solution in the field of solid-state dosimetry is illustrated by simulating the experimental thermoluminescence response curves obtained from LiF:(Mg,Ti)-phosphor-coated borasilicate glass, for the special case of heating with a CO₂-laser beam that has a uniform and square intensity profile: In effect, we solve the diffusion equation experimentally.

The Green-function solution of the transient diffusion equation was previously reported^{1,2} for the case of a semi-infinite two-layer system heated by a localized laser beam of Gaussian or circularly uniform intensity profile. The solution was valid for that time $t < t_p$, where t_p was the pulse duration. The usefulness of the solution was illustrated by its application to laser heating with a cw laser beam in the field of thermoluminescence (TL) dosimetry,¹⁻⁵ where phosphor-coated borasilicate glass comprised the two-layer system. The predicted and experimental response was compared for a wide range of experimental conditions. Accepted literature values were used for the material parameters except for a parameter combination B (defined herein), which was obtained by an independent measurement.⁴ In fitting theory and experiment, B , the only adjustable parameter, agreed with its measured value to within the experimental error. However, in prior work, the TL response was monitored only during the pulse duration t_p , when the source term is "on" in the diffusion equation. Herein, we consider the response of those same samples but follow their response for some time after the laser is turned off. The generation term is now "off" in the transient diffusion equation. As well, the original solution was only valid for laser heating profiles that had either a Gaussian or a circularly uniform intensity profile: a circular spot. In this note, we extend the Green-function solution^{1,2} to times after the laser is turned off. We then illustrate our procedure for analyzing the TL response obtained experimentally using a square heating "spot" in terms of the heating-rate solution for a circular spot, yielding, in effect, a method to solve the diffusion equation experimentally.

The original solution to the transient diffusion equation in cylindrical coordinates (r,z) for a two-layer system of total thickness $L = l_1 + l_2$ yielded a heating rate as a function

of time, t , which is denoted herein as $r_h(r,z,t)$. It is valid for the boundary conditions given as follows:

(1) The two-layer slab is infinite in radial direction and $T(r,z,t) \rightarrow T_0$ as $r \rightarrow \infty$.

(2) No heat loss occurs at the boundaries; i.e., $\partial T_i / \partial z = 0$ at $z = 0$ ($i = 1$) and $z = L$ ($i = 2$).

(3) At the interface ($z = l_1$), $T_1 = T_2$, and $k_1 \partial T_1 / \partial z = k_2 \partial T_2 / \partial z$.

The initial conditions are $T_i(r,z,t) = T_0$; i.e., room temperature, when the laser is turned on at $t = 0$.

Correcting for the reflection loss at the front surface at $z = 0$, the source functions become for $0 < t < t_p$

$$g_1(r,z,t) = \mu_1 (1 - R_1) (P^* / \pi \omega^2) \exp(-\mu_1 z) H(\omega - r)$$

and

$$g_2(r,z,t) = \mu_2 (1 - R_1) (1 - R_2) (P^* / \pi \omega^2) \times \exp[-\mu_1 l_1 - \mu_2 (z - l_1)] H(\omega - r),$$

where P^* is the total laser power (not the power density) incident on the front surface, H the Heaviside step function, R_i the reflectivity and μ_i the absorption coefficient of layer i , and ω the radius of the uniformly circular beam. The rate $r_h(r,z,t)$ is valid only for times $t < t_p$ where t_p is the time the laser is "on". If $R_H(r,z,t)$ denotes the heating rate for any time t where $t > t_p > 0$, then it is readily shown that

$$R_H(r,z,t) = r_h(r,z,t) - r_h(r,z,t - t_p) * H(t - t_p). \quad (1)$$

For the case of a thin phosphor layer on a thicker glass substrate heated through the phosphor, $r_h(r,z,t)$ was given explicitly by

$$r_h(r,z,t) = (BP^* / \omega^2) Q(r,t) \times \left(1 + N_0 \sum_{m=1}^{\infty} \cos(\eta_m z) \exp(-\alpha \eta_m^2 t) / [N_m (1 + \eta_m^2 / \mu_2^2) \cos(\eta_m l_1)] \right)^{-1}.$$

We further have

^{a)} Present address: The Singer Company, Singer-Link-Miles, 8895 McGaw Road, Columbia, MD 20145.

$$\epsilon = (1 - R_1) [1 - (1 - R_2) \exp(-\mu_1 l_1 - \mu_2 l_2) - R_2 \exp(-\mu_1 l_1)] / \pi N_0,$$

$$N_0 = (1/\alpha) \sum_{i=1}^2 k_i l_i,$$

and

$$N_m = \frac{1}{2\alpha} \sum_{i=1}^2 k_i l_i [1 + \sin(2\theta_i)/2\theta_i] \cos^2(\theta_i),$$

with

$$\theta_i = \eta_m l_i, \quad Q(r, t) = P(\omega/\sqrt{2\alpha t}, r/\sqrt{2\alpha t}),$$

k_i the thermal conductivity of the layers, and $\alpha_1 = \alpha_2 = \alpha$ their approximately equal thermal diffusivity.

$$P(\omega, r) = \int_0^\infty \omega' d\omega' I_0(\omega', r) \exp[-(\omega'^2 + r^2)/2]$$

is called the circular coverage function. The parameters η_m ($m = 1, 2, \dots$) are obtained from

$$k_1 \tan(\theta_1) + k_2 \tan(\theta_2) = 0,$$

which arises from the boundary conditions.

Under certain experimental conditions, it is possible to obtain a fast and linear temperature rise. In fact, this ability has been used to measure the luminous efficiency of a number of different phosphors.^{5,6} Then $r_n(r, z, t)$ is a constant and from Eq. (1), $R_H(r, z, t) = 0$ is obtained for $t > t_p > 0$. Equation (1) was derived assuming that the intensity profile of the heating spot was circularly uniform. This solution for small times is not amenable to computation. However, for short times, i.e., times less than $1 \mu\text{s}$, there is no (useful) TL response, and a good approximation is a zero heating rate for this time interval. We also note that a TL response curve

simulated with this expression for the heating rate has its maximum at a time dependent on B .

The TL response of a dosimeter configuration, with the heating rate given by Eq. (1), is simulated with the prior procedure.² It requires only that the parameter B , the laser power, and the cutoff time be chosen and that an effective ω be used. The TL response of a dosimeter configuration heated with a square spot of side 2ω , is readily obtained experimentally. This response lies between that obtained for the inscribed circular spot of radius $\omega_i = \omega$ and of that for the circumscribed circular spot of radius $\omega_c = \sqrt{2}\omega$. We ignore, for the present note, the temperature dependence of the thermal conductivities k_i . It has also been shown that the z dependence is minimal for a two-layer system when, as is the case, one layer is weakly absorbing ($\mu_1 \sim 40 \text{ cm}^{-1}$, $\mu_2 \sim 10^4 \text{ cm}^{-1}$). This remains true for times $t > t_p$, so we choose the value $z = 0.5l_1$.

The experimental setup and sample preparation^{1,2} have been described fully. We have repeated previously reported work² using a modified version of the TL reading apparatus: the circular aperture was removed (see Fig. 1 in Ref. 1) to produce a square "spot" of area $3 \times 3 \text{ mm}^2$. Figure 1 illustrates the typical TL response for several different powers obtained for those same samples² but for a variety of laser cutoff times. TL response curves for $t = t_p$ are very similar to those previously reported.²

The TL response for a power of 9.75 W was obtained with a cutoff occurring near the maximum. A fit to this data is obtained with Eq. (1) with a circular radius of $\omega_c = 0.3/\sqrt{\pi} \text{ cm}$. Only the parameter combination B was adjusted to match the location of the maximum response. The normalized TL response obtained with a uniform inten-

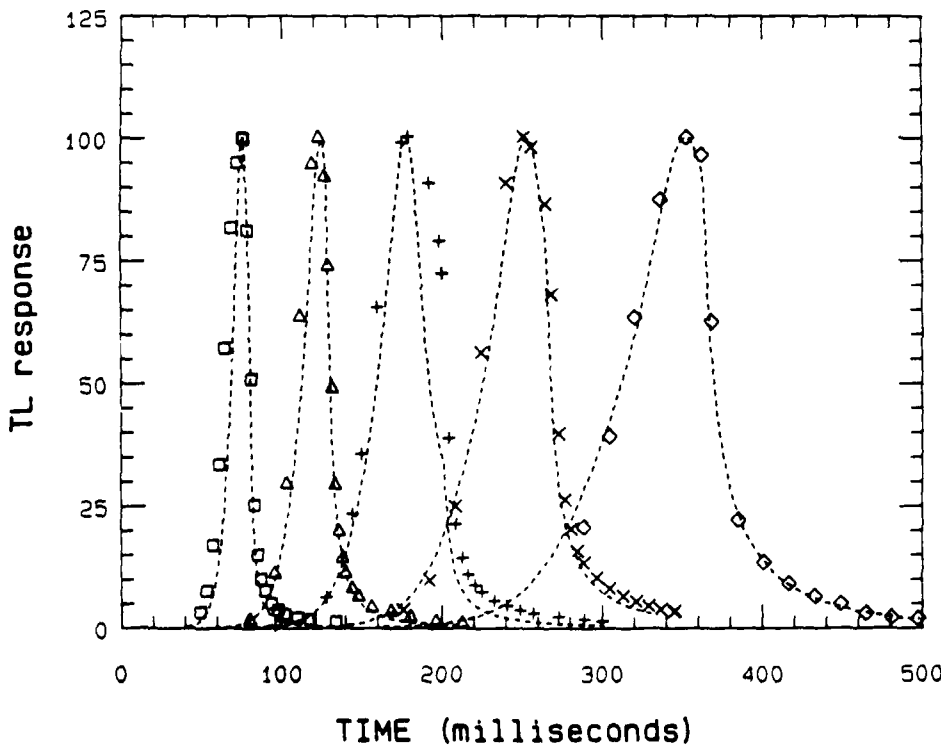


FIG. 1. Thermoluminescence response curves measured (data points) and calculated (dashed lines) with a uniform laser beam of $3 \times 3 \text{ mm}^2$ profile with the material parameters described in Ref. 2. The laser beam impinges on the phosphor surface. The curves from left to right were obtained with laser beam powers of 9.75, 6.5, 4.88, 3.25, and 2.44 W, and corresponding B values of 9.78, 9.13, 8.61, 9.13, and $8.76 \text{ K cm}^2/\text{J}$. The laser cutoff times are 80, 128, 200, 251, and 362 ms, respectively.

sity profile should be independent of the size of the heating "area" for semi-infinite media. Similarly, one should obtain the same simulated response independent of the choice of the radius ω . In this regard, we note, for example, that the simulated response for 2.44 W, which is shown in Fig. 1, is also obtained with ω equal to ω_i or to ω_c . However, new values are obtained for B ($B \pm 2\%$, respectively, with B the value for $\omega = \omega_s$). We can eliminate those values of B outside the limits of experimental error for those values of ω greater than ω_c or less than ω_i and get a measure of the usefulness of this approximation. The measured value of B was determined⁴ to be $10.7 \pm 25\% \text{ K cm}^2/\text{J}$. The values of B obtained by fitting are within this range (the best fit being obtained with $\omega = \omega_s$).

As Fig. 1 illustrates, it is generally found that the fit to the actual response is adequate, although there are times when it is poor, as shown for the case of 4.88 W. It is not clear yet whether this is due to a nonuniform phosphor coating or other factors.^{1,2} In general, the simulated response is enveloped by the experimental response, which indicates that the temperature dependence of the thermal conductivities should be included in the comparison.²

We have extended the previous solution^{1,2} of the diffusion equation to all times, albeit for a specially considered two-layer system, and we have illustrated its usefulness by applying it in the field of solid-state dosimetry. While we have considered a composite that was heated through the

phosphor layer, the above analysis is readily extended to such a composite heated through the glass layer. It appears then that laser heating of practical dosimeter configurations consisting of phosphor-coated glass are adequately described by Eq. (1) above provided only that the glass is a much better absorber than the phosphor. The idea of using TL response to solve the diffusion equation is novel. It is limited in this instance by experimental error and, because of the large uncertainty in B , the present method is not a very sensitive test. Perhaps a better composite system can be found: one in which the temperature dependence of all the material parameters is known. Finally, we note, that the approximation used herein is probably valid for any shape of the heating "spot."

We thank Norm L. Henry, of the Physics Division of NRC, for many helpful discussions. This work was sponsored, in part, by the Office of Naval Research under Contract No. N00014-82-K-0529.

¹ A. Abtahi, P. Braunlich, and P. Kelly, *J. Appl. Phys.* **60**, 3417 (1986).

² P. Kelly, A. Abtahi, and P. Braunlich, *J. Appl. Phys.* **61**, 738 (1987).

³ P. Braunlich, J. Gasiot, P. J. Fillard, and M. Castagne, *Appl. Phys. Lett.* **39**, 769 (1981).

⁴ A. Abtahi, P. Braunlich, P. Kelly, and J. Gasiot, *J. Appl. Phys.* **58**, 1626 (1985).

⁵ A. Abtahi, P. Braunlich, T. Haugan, and P. Kelly, *Radiat. Prot. Dosim.* **17**, 313 (1986).

⁶ A. Abtahi, T. Haugan, and P. Kelly, *Radiat. Prot. Dosim.* **21**, 211 (1987).

Part II: Summary of Work on CaSO₄:Sm

The final phase of this research program was concerned with the optical stimulation of dose-related luminescence from a traditional thermoluminescent dosimetry phosphor. This was achieved with some degree of success with visible laser stimulation of a rare-earth doped CaSO₄ phosphor, CaSO₄:Sm. The radiation-induced signal is also optically erasable.

The essential features of the process are that normally the samarium occurs in the triply ionized (3+) state, but exposure of the phosphor to ionizing radiation (we tested the process with ultraviolet and gamma radiation) results in a dose-dependent partial conversion of Sm³⁺ to Sm²⁺ (the samarium ions serve as electron traps).

Rare-earths exhibit characteristic luminescence (the basis of several laser systems) which can be selectively observed with spectroscopic instrumentation. Furthermore, the luminescence spectra of the samarium ions possess excitation bands such that a tunable stimulating light source can more or less selectively excite the Sm²⁺ and Sm³⁺ species. We employed a tunable, cw dye laser to stimulate the Sm²⁺ luminescence spectrum, and an optical multichannel analyzer to record and analyze the emission for dosimetric information.

One interesting feature of the experiment turned out to be that at the chosen stimulation wavelength (573 nm, chosen after studying the excitation spectrum) the Sm²⁺ emission (\approx 600-775 nm) is more accurately described as prompt fluorescence! The ion is excited (by single-photon absorption) to a high level, and radiative relaxation follows promptly. Thus, the readout or dose extraction procedure does not erase or significantly degrade the dose information: the signal is more or less permanently stored until an erase procedure is carried out. The signal can be erased (i.e., the Sm²⁺ can be re-ionized to Sm³⁺) by exposure of the phosphor directly to the output of the cw argon laser (all-lines) that serves as the dye laser pump. A full investigation of the temporal and power dependent characteristics was not carried out. However, over 95% of the signal was

erased within 5 seconds of the onset of exposure to the sample to the erasing light, although most of this decrease occurs within the first 0.5 seconds [see Fig. 23, p. 72 of the Appendix (M.S. thesis, K. W. Wells)].

Surprisingly, attempts to thermally reset the phosphor resulted in the opposite effect occurring: rather than reducing the radiation induced signal, thermal treatment actually increased the Sm^{2+} emission. In a similar fashion, storage of the phosphor for several weeks between irradiation and evaluation also led to an increase of approximately equal magnitude compared with the thermal treatment. The signal does, however, stabilize with either heating or time. We believe the occurrence of this phenomenon is the result of electrons in shallow traps being transferred to Sm^{3+} ions. The fact that heating the phosphor does not erase the fluorescence signal (even up to 600°C for 1 hour) points to the difference between this process and thermoluminescence. The phosphor exhibited a typical TL behavior: a single transient glow curve is obtained upon heating the phosphor through 300°C . Heating the material does not affect those electrons trapped at Sm^{2+} sites.

The optical erasure process is dependent on the specific composition of the phosphor. Three cases were studied: $\text{CaSO}_4:\text{Sm}$ without any co-dopant, $\text{CaSO}_4:\text{Sm}$ co-doped with 500 ppm sodium and a third with 1000 ppm sodium. For all three formulations, the radiation-induced signal was completely erasable with the argon laser. However, we did observe a regrowth of the Sm^{2+} fluorescence in the samples over a matter of hours after the erasure. We believe this to be related to the thermally-induced signal increase discussed above. It does appear that this regrowth can be controlled. The greatest signal regrowth occurred in the phosphor that was not co-doped with sodium. Addition of 500 ppm sodium cut this regrowth by approximately a factor of four, and the 1000 ppm sodium formulation reduced the regrowth by more than a factor of ten below the case where no sodium was intentionally added. (Refer to Fig. 17, p. 64 of Appendix) Thus, it appears that approximately equal quantities of Sm and Na are required to eliminate the regrowth. We did not, however, pursue this point further, and the optimum

formulation to eliminate the regrowth is as yet undetermined, but we believe attainable. Apparently, the $\text{Sm}^{(3+)}$ dopant, which substitutionally replaces the $\text{Ca}^{(2+)}$ in the phosphor, needs to be compensated with a singly positive ion. This compensation will occur naturally, or it can be controlled by purposely adding an ion such as Na^+ . We believe that in this case, the Na^+ provides deep, stable electron traps that hold electrons which would otherwise be transferred to Sm^{3+} to form Sm^{2+} , thus causing a signal regrowth.

Dosimetrically, the experimental system was found to be very inefficient for collecting the radiation-induced fluorescence signal, and thus the apparent sensitivity of this process is at a level of about 0.01 Gray (1 rad). However, the goal was not to engineer a high sensitivity dosimetry system but rather to study a possible process of optical stimulation for recovering dosimetric information on which to base further work. The system can certainly be vastly improved to improve the dosimetric performance.

One advantage of optical stimulation (that is, as opposed to thermal stimulation, as in laser-heated thermoluminescence) is that there is no diffusion of heat. Thus, the region stimuable with a visible laser can be as small as a few microns in diameter, although we have not yet shown that this is practical. Thus, in principal, the "pixel" size is small enough to produce high resolution images, or as an erasable optical data recording medium, since the phosphor can be "written" on and read out with optical beams. A crude imaging experiment was performed and is described in Chapter 5 of the Appendix.

Thus, the final year of this ONR sponsored program was successful in achieving its aim: to show that a commonly used thermoluminescence dosimetry phosphor can be stimulated by optical means to yield dosimetric information and also can be returned to its initial state by an optical beam to prepare it for reuse. The use of a common thermoluminescent material is important for the eventual acceptance of optically stimuable luminescence in personnel radiation dosimetry. In addition, the utility of optical stimulation will include high resolution radiation field and dose distribution mapping (e.g., in radiological phantoms) and make remote-fiber optic dosimetry more straightforward.

Further, since there is no glow curve involved in extracting the dosimetric information, there is no apparent need to perform lengthy, high temperature annealing procedures to prepare the phosphor for reuse. For this reason, it is feasible to encase the phosphor in transparent, hydrogenous, low melting point plastic (e.g., polyethylene) to serve as a proton irradiator for neutron dosimetry (protons are knocked out of the plastic by fast neutrons and directly excite the phosphor). Since no heating is necessary, the phosphor can be read out while still encased. The results of this investigation are very promising for future developments in radiation dosimetry.

Publications

1. P. Braunlich, S. C. Jones, A. Abtahi, and M. deMurcia, "Heating of Continuous Thermoluminescent Layers with Localized Laser Beams," *Radiation Protection Dosimetry* **6**, 83-86 (1984).
2. P. Kelly, P. Braunlich, A. Abtahi, S. C. Jones, and M. deMurcia, "Thermoluminescence Kinetics at the Extreme Heating Rates Possible with Thermal Laser Stimulation," *Radiation Protection Dosimetry* **6**, 25-28 (1984).
3. G. Brost, P. Horn, and A. Abtahi, "Convenient Spatial Profiling of Pulsed Laser Beams," *Appl. Optics* **16**, 38-40 (1985).
4. A. Abtahi, P. Braunlich, P. Kelly, and G. Gasiot, "Laser-Stimulated Thermoluminescence," *J. Appl. Phys.* **58**, 1626 (1985).
5. A. Abtahi, P. Braunlich, and P. Kelly, "Theory of Transient Temperature Response of a Two-Layer System Heated with a Localized Laser Beam," *J. Appl. Phys.* **60**, 3417 (1986).
6. P. Kelly, A. Abtahi, and P. Braunlich, "Laser-Stimulated Thermoluminescence II," *J. Appl. Phys.* **61**, 738 (1987).
7. A. Abtahi, P. Braunlich, T. Haugan, and P. Kelly, "Investigation of Thermoluminescence Efficiencies at High Laser Heating Rates," *Radiation Protection Dosimetry* **17**, 313-316 (1986).
8. A. Abtahi, T. Haugan, and P. Kelly, "Investigation of the Dosimetric Properties of $MgB_4O_7:Dy$ under Laser Heating," *Radiation Protection Dosimetry* **21**, 211 (1987).
9. J. F. Young, P. Kelly, A. Abtahi, P. Braunlich, and S. C. Jones, "Transient Solutions of the Diffusion Equation for Composite Systems Heated with a Laser Beam," *J. Appl. Phys.* **60**, 5627 (1989).

Invited Presentations at Scientific Conferences

1. P. Braunlich and P. Kelly, "Laser-Stimulated Exoelectron Emission," 8th International Symposium on Exoelectron Phenomena on Applications, August 25-29, 1985, Osaka, Japan (published in *Japan. J. Appl. Phys.* **24**, 38-42 (1985)).
2. P. Braunlich, "Present State and Future of TLD Laser Heating," 9th International Conference on Solid State Dosimetry, November 6-10, 1989, Vienna, Austria. Accepted for publication in *Radiation Detection Dosimetry* (1990).
3. P. Braunlich, "Laser-Heated Thermoluminescence Dosimetry," 8th Conference on Radiation Physics, January 1990, Bhabha Atomic Research Center, Bombay, India.

Patent Disclosures

1. P. Braunlich and A. Abtahi, "Real-Time Radiation Imaging Based on Color-Switching ZnS:Dy Infrared Stimulable Phosphors" (submitted to the Patent Office of Washington State University in 1988—no action taken).
2. K. B. Wells, S. C. Jones, P. F. Braunlich, "Optically Stimulated Fluorescence in CaSO₄:Sm." The subject of this invention is an optically stimulable dosimetric phosphor that can be read at visible wavelengths, annealed with UV and that stores the dose information over long periods of times—a genuine optically stimulable phosphor for radiation dosimetry. (Submitted to the Patent Office of Washington State University in July 1990.)

Theses

1. Abdollah Abtahi, Ph.D., 1986
"Laser Stimulated Thermoluminescence"
2. Timothy Haugan, M.S., 1986
"Dependence of the TL Efficiency on the Heating Rate"
3. Keith B. Wells, M.S., 1989
"Optically Stimulated Fluorescence in Samarium Doped Calcium Sulfate"

List of Graduate Students and Research Personnel Supported

1. Abdollah Abtahi; Ph.D., Physics
2. Timothy Haugan; M.S., Physics
3. Keith W. Wells; M.S., Physics
4. Michael Runkel; Research Assistant
5. George Brost; Research Assistant
6. Scott C. Jones; Research Physicist/Assistant Professor

List of Guest Scientists (unsupported)

1. Dr. Mario deMurcia; Montpellier, France
2. Professor Dr. Jean Gasiot; Montpellier, France
3. Dr. Paul Kelly; National Research Council, Ottawa, Canada